

Application of Geof foam in Thermal Encapsulation of Foundations

Project Leader: Hiramani R. Chimaurya

Team: Clay Caldwell, Nripojyoti Biswas, Gustavo
Hernandez Martin

PI: Anand J. Puppala

Professor | A.P. and Florence Wiley Chair
Director – Center for Infrastructure Renewal

Closed Meeting

TAMU Site Proprietary

NSF IUCRC CICI TAMU SITE
NSF IUCRC CICI - IAB Spring 2024 Meeting

May 23, 2024

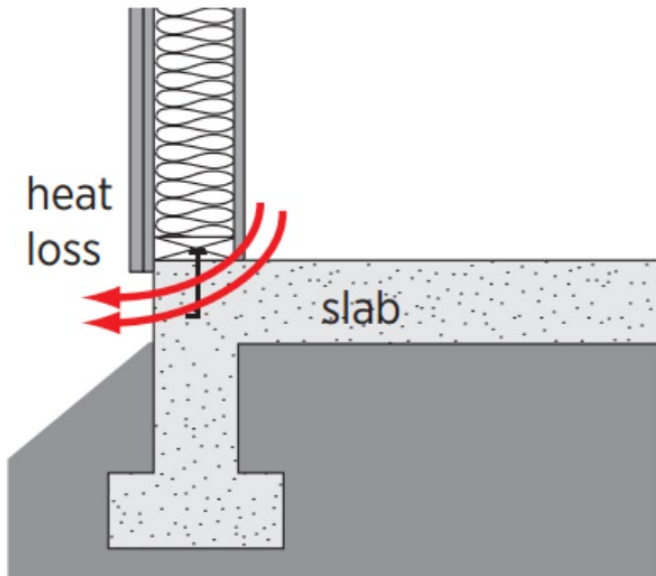


Presentation Outline

- ❑ Introduction
- ❑ Test Methodology
- ❑ Previous GBF & GAF Tests
- ❑ R-130 Geofam Around Footing (GAF) Tests
 - GAF-2 in. R-130 Test
 - Indoor Temperature: Control vs GAF
 - Slab Temperature: Control vs GAF
- ❑ Results Summary
- ❑ Conclusions

Introduction

- ❑ Temperature fluctuations inside the dwellings typically occur from advection, diffusion and radiation at foundation superstructure joints
- ❑ About 15% of all heat loss in a home is through floors or basements
- ❑ Thermal Encapsulation using Geofoam
 - Research Plan
 - Laboratory Testing Setups

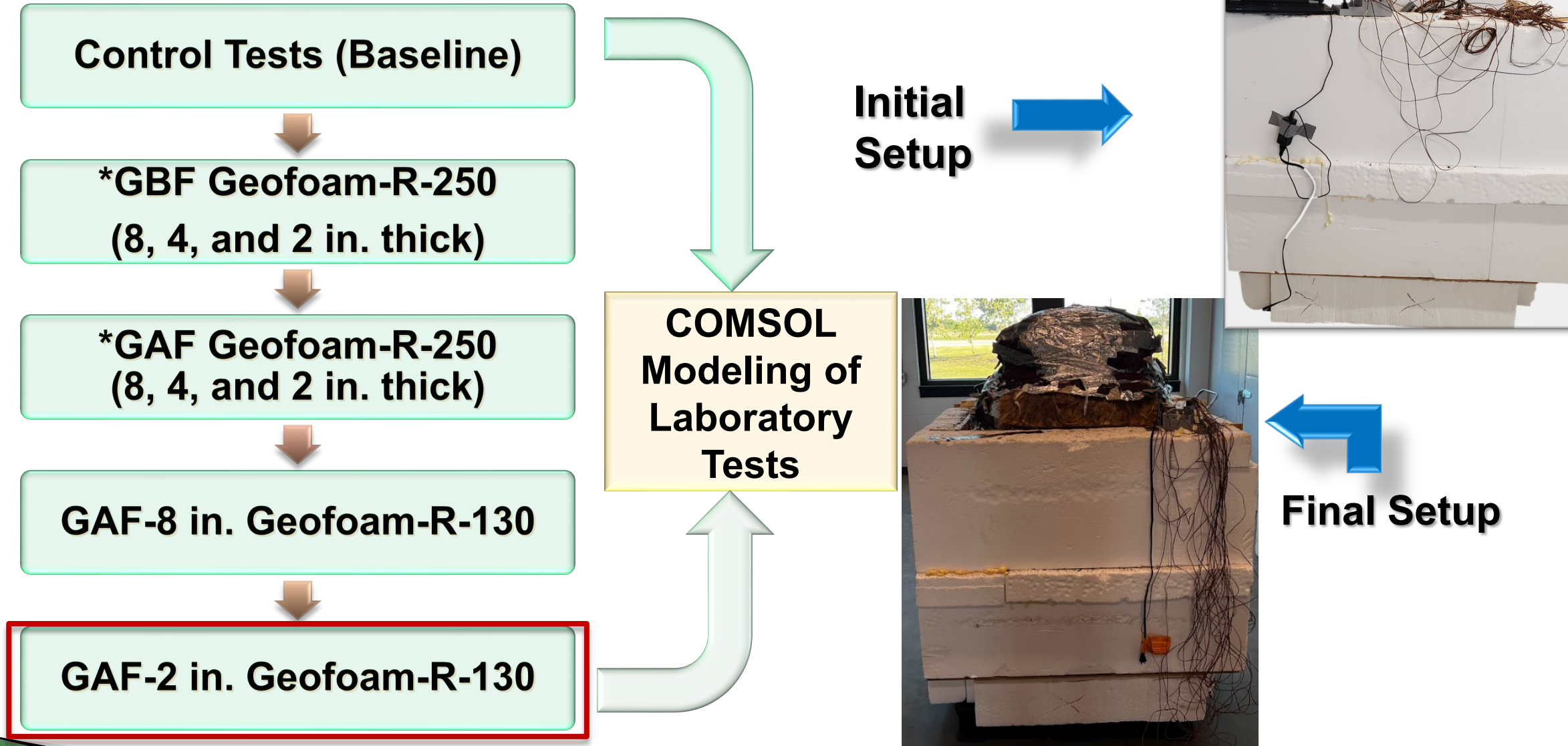


Heat loss



The stack effect

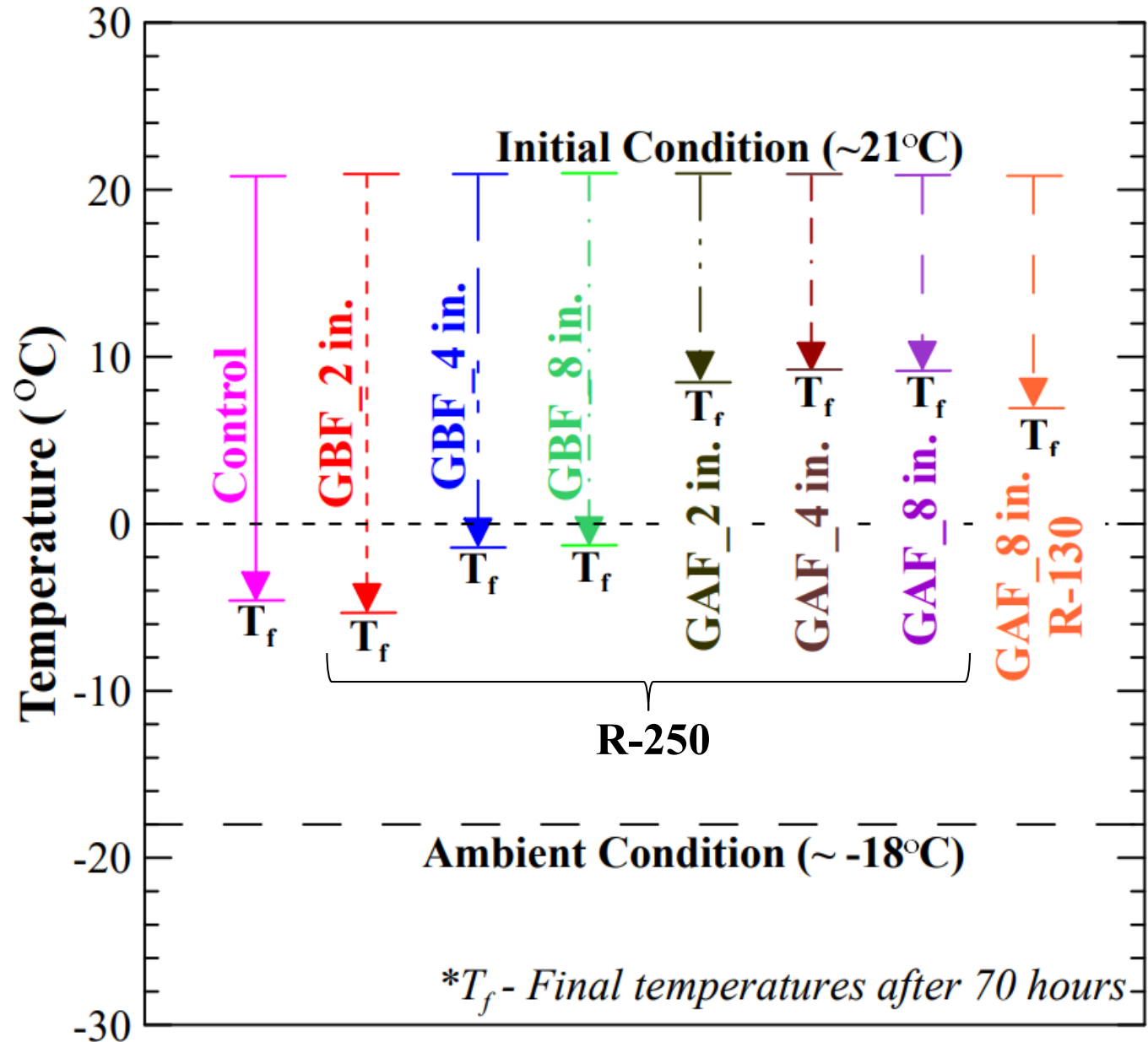
Test Methodology



*GBF: Geofoam Below Foundation
GAF: Geofoam Around Foundation

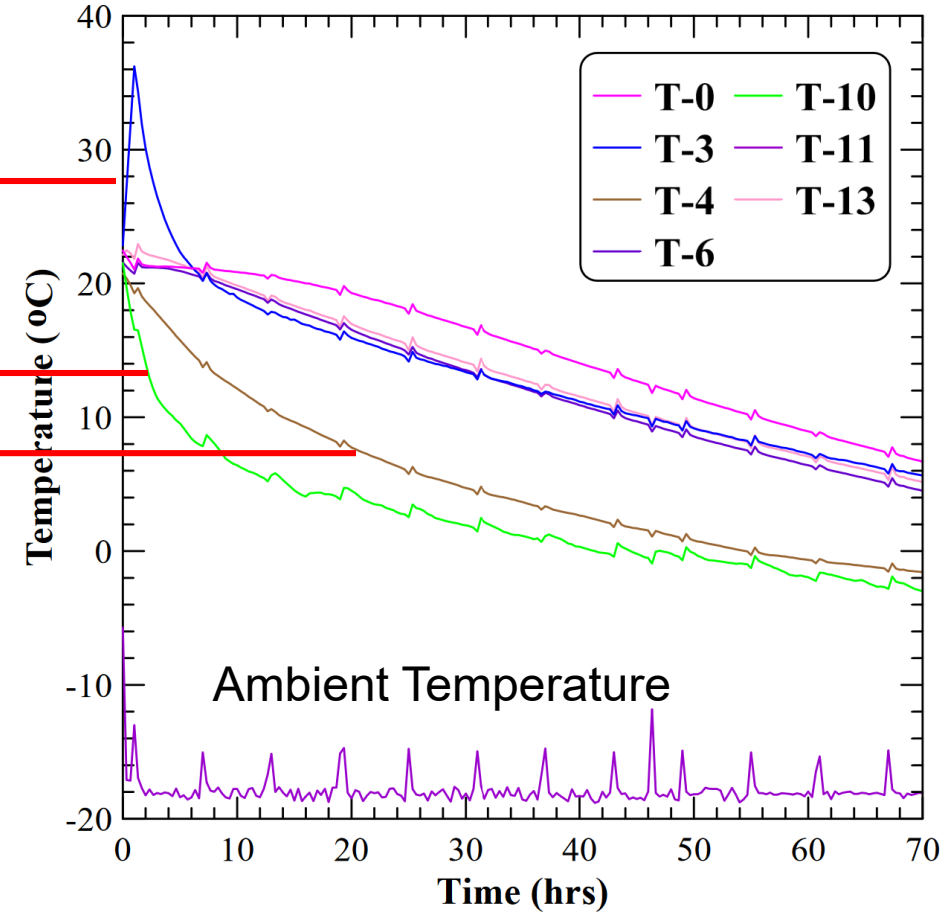
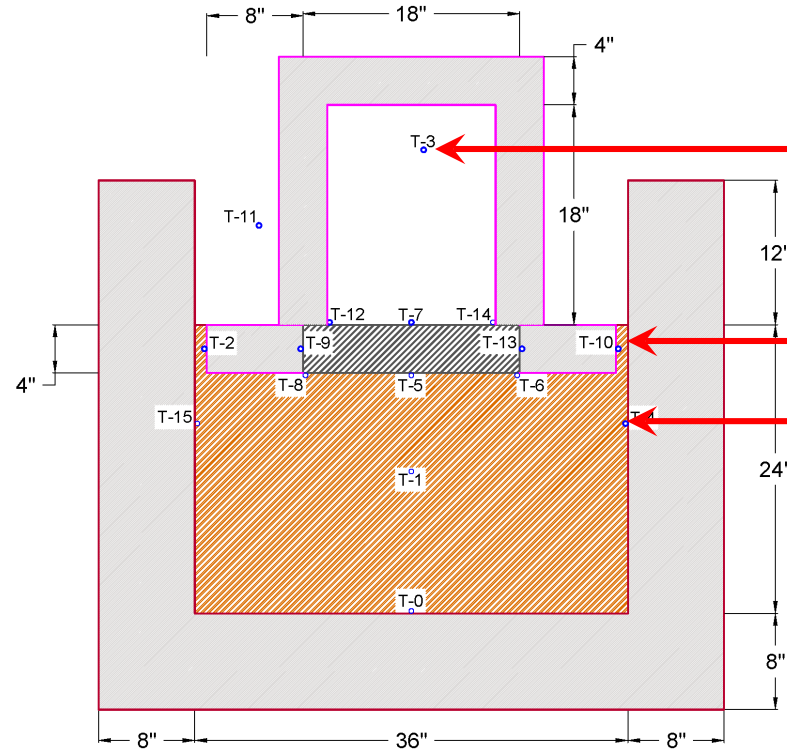
Previous GBF & GAF Tests

- GAF configurations significant outperform all GBF tests
- GAF sections $>8^{\circ}\text{C}$ warmer indoor temperature than GBF sections and $>10^{\circ}\text{C}$ warmer than Control section
- Not much difference in performance for thicker insulation \rightarrow 2 in. GAF most efficient



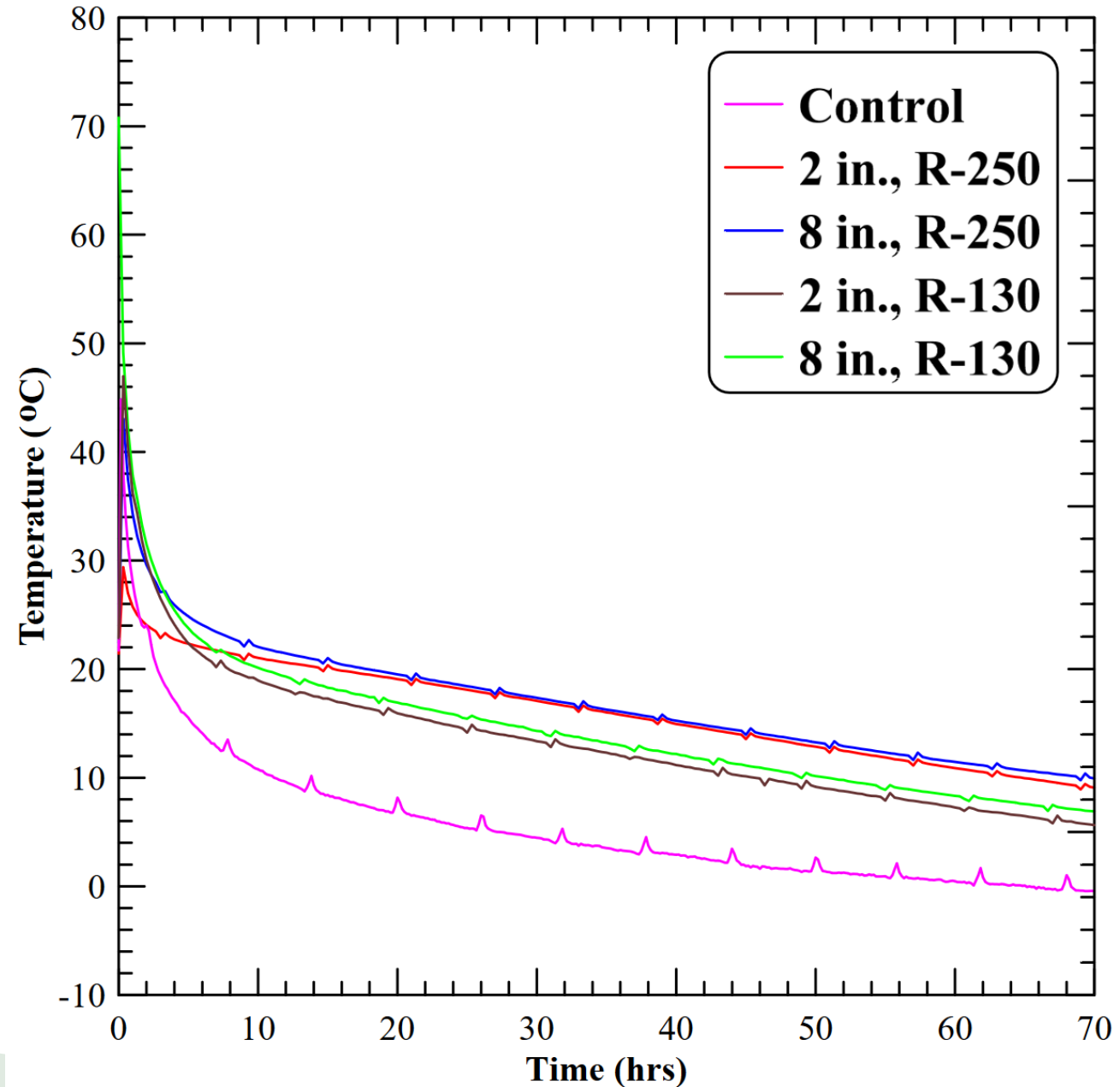
GAF-2 in. R-130 Test

- ❑ Significantly warmer indoor temperature compared to control test ($>5^{\circ}\text{C}$) warmer
- ❑ Increased temperature observed within the slab and superstructure – reduced heat loss
- ❑ Side walls – coldest



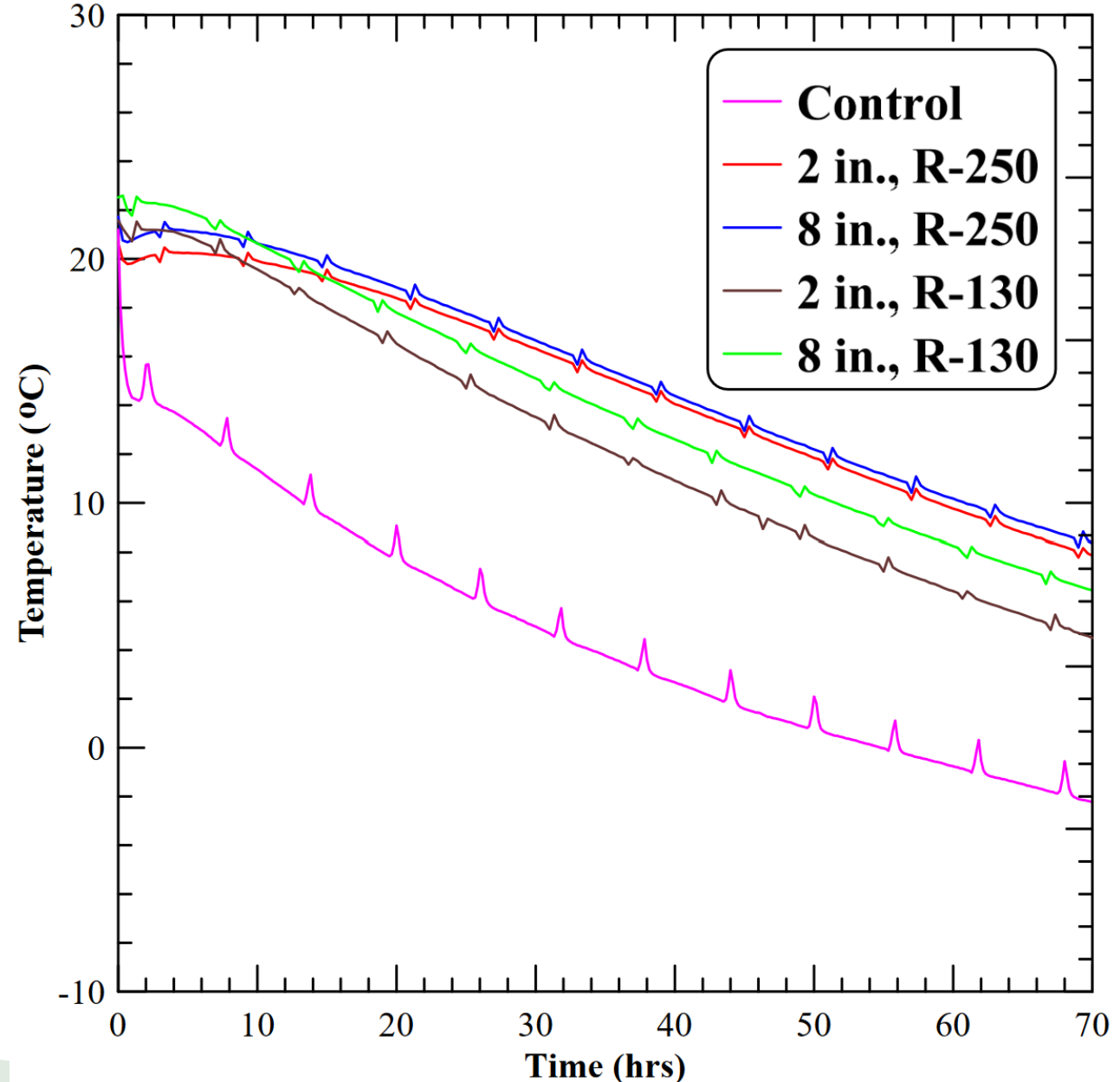
Indoor Air Temperature: Control vs GAF

- ❑ Similar trend of reduced heat loss observed in all 4 GAF tests
- ❑ Lower R-values led to cooler indoor temperatures
- ❑ R-250 sections $> 1.5^{\circ}\text{C}$ warmer than R-130 section
- ❑ 2 in. thick R-130 geof foam may be least efficient GAF configuration



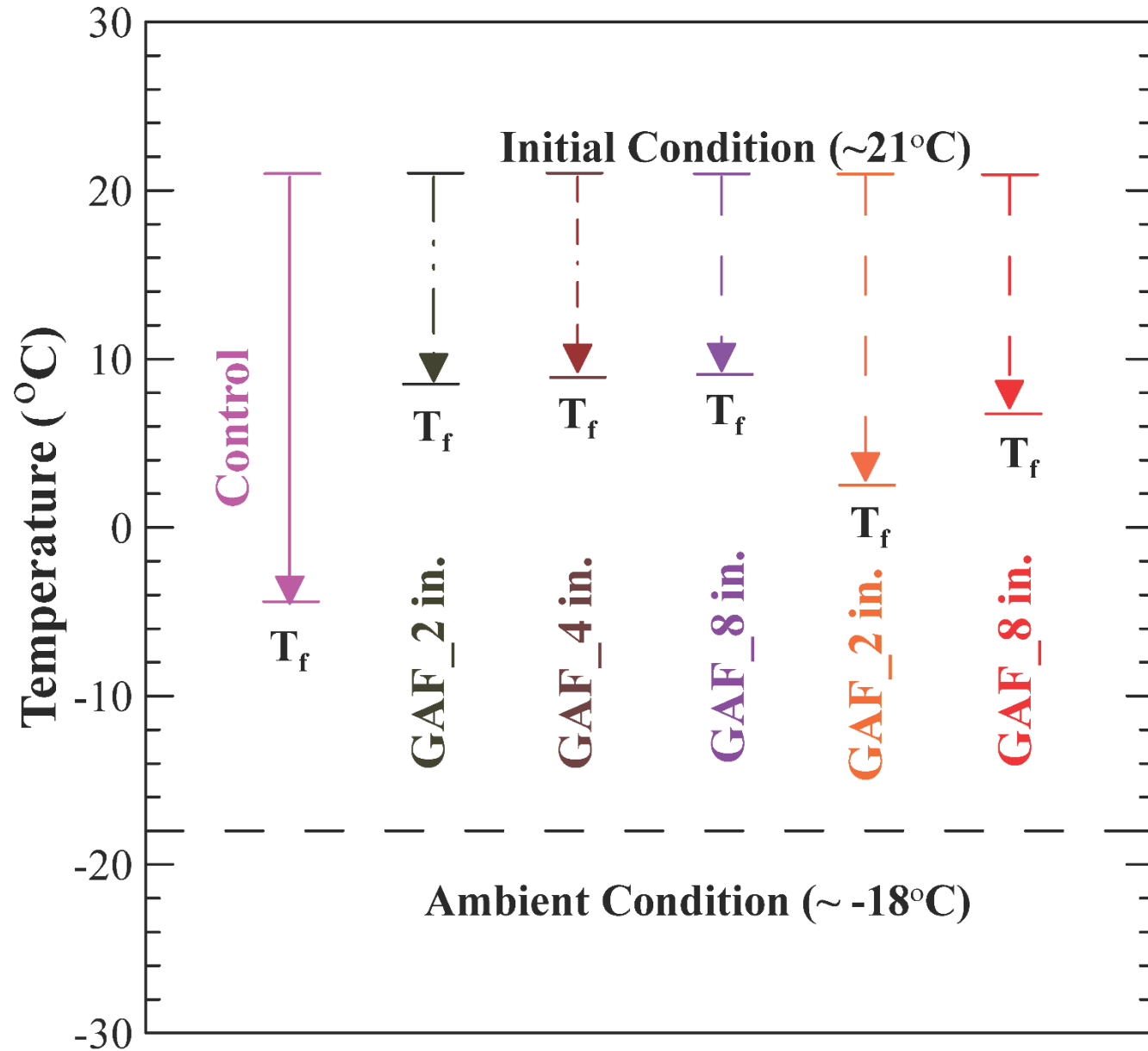
Slab Temperature: Control vs GAF

- ❑ All GAF sections $> 10^{\circ}\text{C}$ warmer slab temperature than Control
- ❑ Lower R-values led to cooler slab temperatures
- ❑ 8 in. R-250 sections $> 2^{\circ}\text{C}$ warmer than 8 in. R-130 section
- ❑ 2 in. R-250 sections $> 6^{\circ}\text{C}$ warmer than 2 in. R-130 section



Results Summary

- ❑ GAF-2 in. R-250 section had $>4^{\circ}\text{C}$ warmer slab temperature than GAF-2 in. R-130 section
- ❑ GAF-8 in. R-250 section had $>2^{\circ}\text{C}$ warmer slab temperature than GAF-8 in. R-130 section
- ❑ GAF- 8 in. R-250 section had $>2^{\circ}\text{C}$ warmer slab temperature than GAF-8 in. R-130 section



Conclusions

- ❑ Better performance of GAF → Heat lost to ambient air controlling factor
- ❑ Thinner insulation with higher R-value performed better than thicker insulation with lower R-value
- ❑ GAF-2 in. thick R-250 outperformed GAF-8 in. thick R-130
- ❑ Thermal properties and insulation configuration had more influence than thickness of geof foam
- ❑ Influence of insulation thickness was higher for lower grade geof foams
- ❑ 2 in. thick R-250 in GAF configuration could be an efficient option

Design and Testing of IFI Geosynthetic Products

Project (Leader): Krishneswar Ramineni

Team: Nripojyoti Biswas, Avinash Gonnabathula, and Md Ashrafuzzaman Khan

PI: Anand J. Puppala

Professor | A.P. and Florence Wiley Chair

Director – Center for Infrastructure Renewal

Closed Meeting

TAMU Site Proprietary

NSF IUCRC CICI TAMU SITE
NSF IUCRC CICI - IAB Spring 2024 Meeting



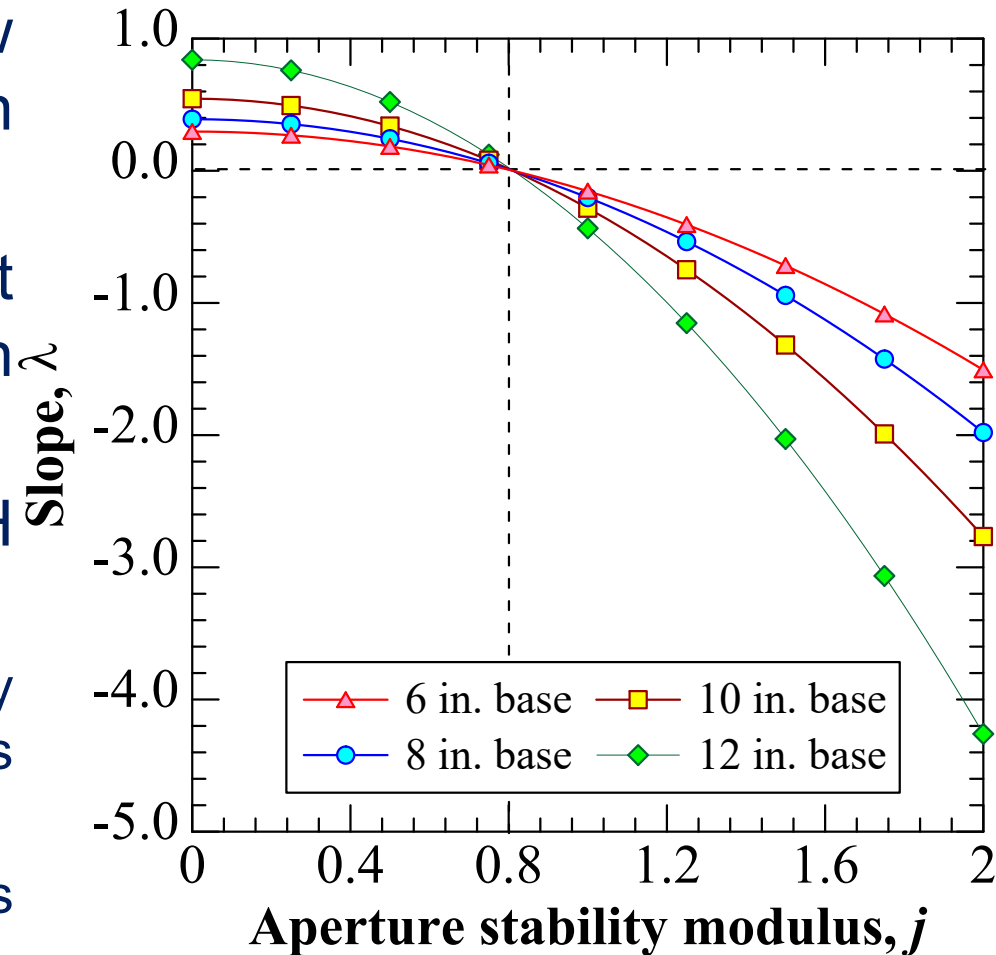
Presentation Outline

- ❖ Introduction and Background
- ❖ Objectives
- ❖ Experimental Program
- ❖ Test Results and Trends
- ❖ Unpaved Base Layer Design
- ❖ Design Charts
- ❖ Limitations
- ❖ Summary
- ❖ Future Work



Introduction and Background

- ❑ Pavements built over poor subgrade soils → low bearing capacity, distress and construction issues
- ❑ Geosynthetics → Improve pavement performance → High modulus geogrids can work on weak subgrades
- ❑ Limitations of existing design method (G-H method)
 - Applicable only to geogrids with aperture stability modulus, j below 0.8 m-N/deg (experimental values used in the development are less than this value!)
 - Assumes the initial stress distribution of first cycle as constant
- ❑ Need to update the calibration equation and develop design charts



Slope vs Aperture stability modulus graph based on G-H equation

Objectives

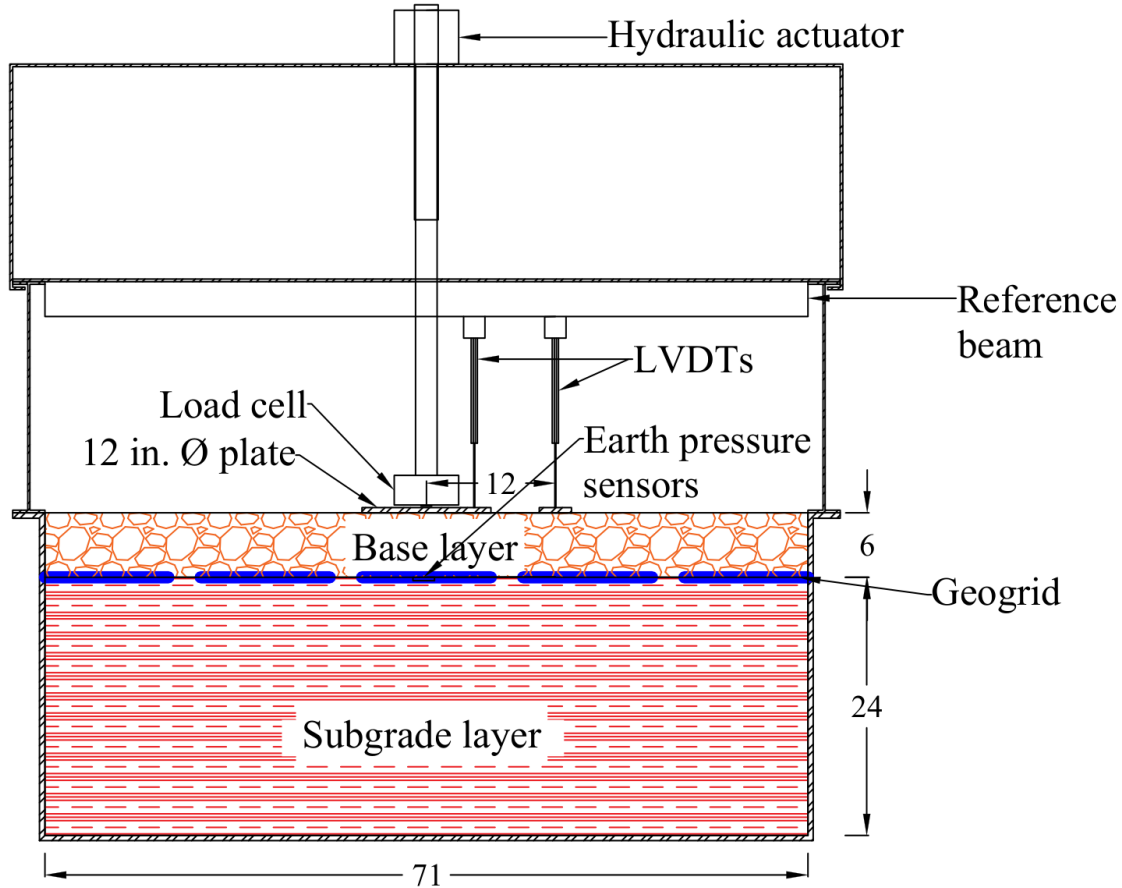
The objectives of the current study are:

- ❑ **Phase 1 Part 1** Objective I : Performing repeated load tests on geosynthetic reinforced base layers built on different weak subgrades (12-inch base sections)
- ❑ **Phase 1 Part 2** Objective II: Development of various design charts and methods for IFI, Inc Geosynthetic Products based on Phase 1 Part 1 results
- ❑ **Phase 1 Part 3** Objective III: Perform non-destructive tests on geosynthetic reinforced unpaved sections and develop numerical model to determine the stiffness properties of different pavement layers in the field.
- ❑ **Phase 2 Part 1** Objective IV: Performing repeated load tests on geogrid reinforced base layers built on different weak subgrades (6-inch base sections)
- ❑ **Phase 2 Part 2** Objective V: Development of various design charts and coefficients for IFI, Inc Geosynthetics products based on Phase 1 Part 1 and Phase 2 Part 1 results



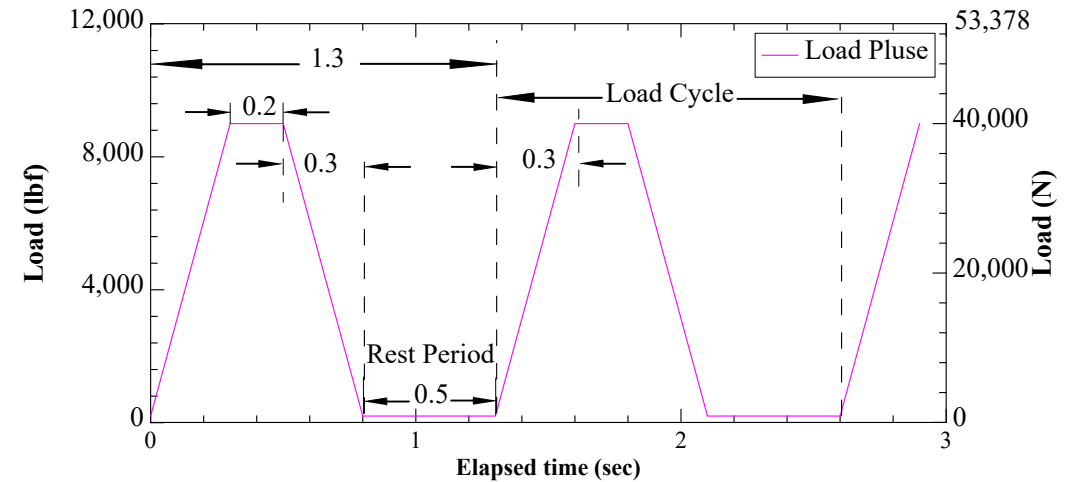
Experimental Program

Large-Scale Repeated Load Testing



Note: All dimensions are in in. (1 in. = 25.4 mm)

Schematic of the large-scale test box



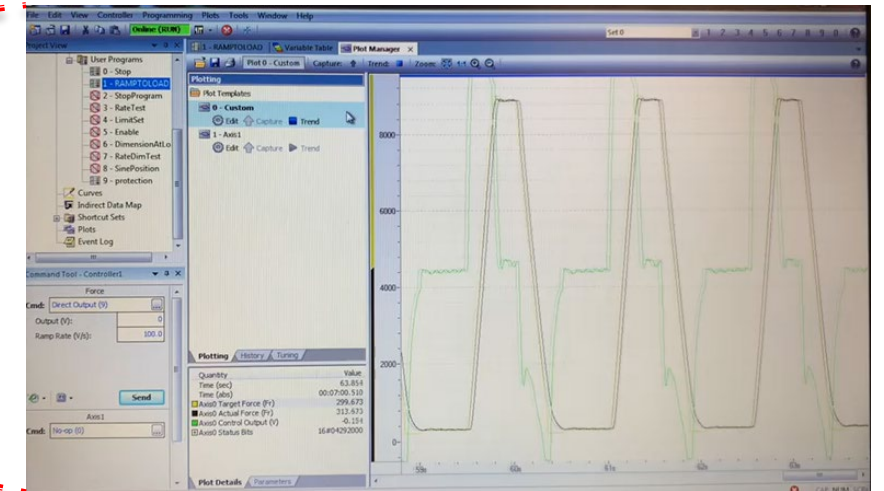
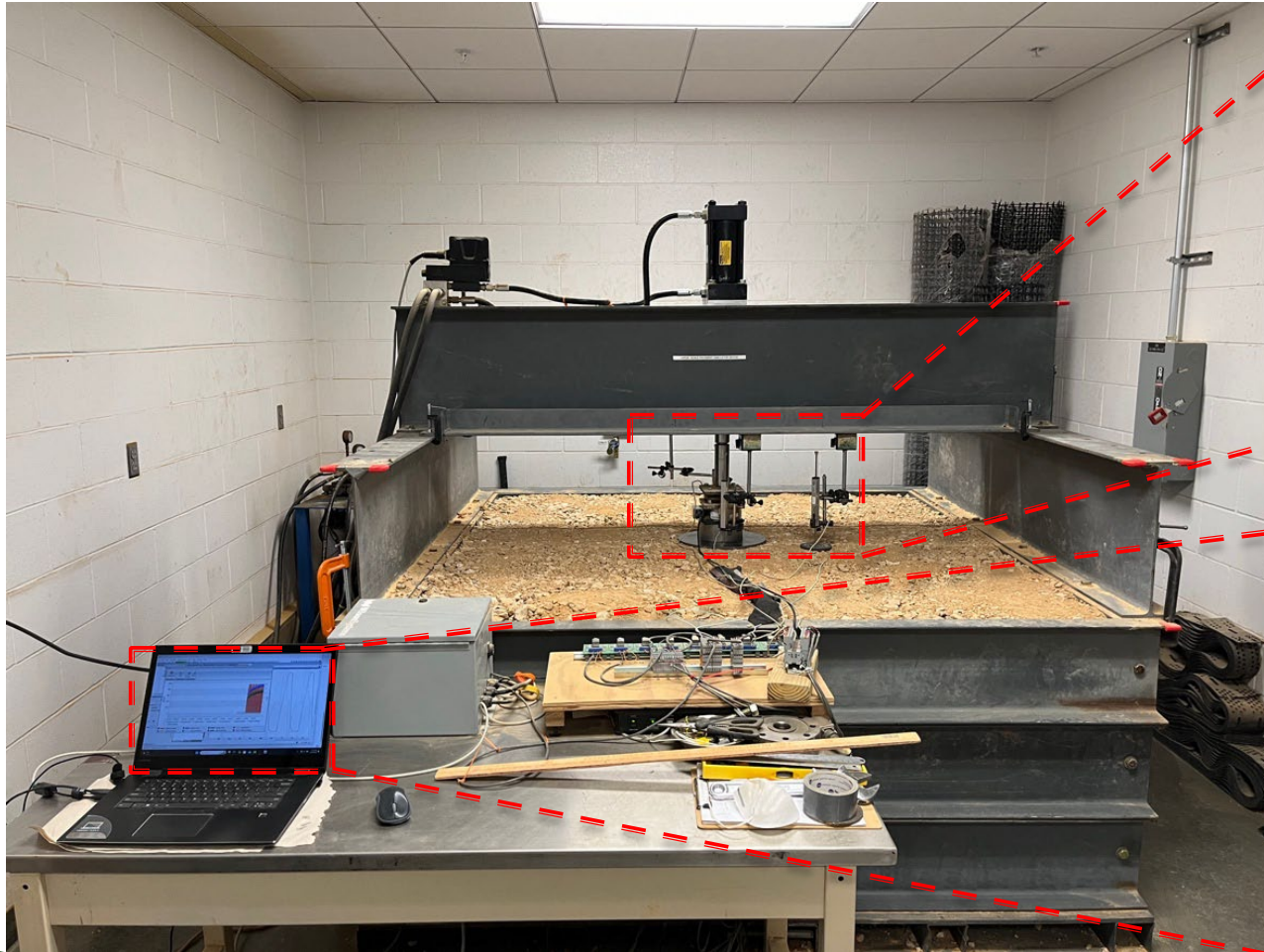
Repeated load pulse

- ❑ Frequency of loading: 0.77 Hz
- ❑ Peak load: 9000 lbf
- ❑ Loading plate diameter: 12 in.
- ❑ Instrumentation: Load cell, pressure sensors, Multiple LVDTs

Reinforcement layer was placed at the interface of base and subgrade layers

Experimental Program

Large-Scale Repeated Load Testing



Experimental Program

Large-Scale Repeated Load Tests Performed on Geocell/Geocomposites

Test ID	(<i>h</i>)	(CBR_{sg})	Geosynthetic type	Geosynthetic material property
12_1_FG6	12 in.	CBR 1	Geocomposite (FG6)	$j = 0.80$ m-N/deg + Non-woven
12_1_GCSP4			Geocell (GCSP4)	4 in. height
12_1_GCSP6			Geocell (GCSP6)	6 in. height
12_1_BL6_GCSP4			Geogrid (BL6) + Geocell (GCSP4)	$j = 0.98$ m-N/deg + 4 in. height
12_1_BL6_GCSP6			Geogrid (BL6) + Geocell (GCSP6)	$j = 0.98$ m-N/deg + 6 in. height
12_3_FG6		CBR 3	Geocomposite (FG6)	$j = 0.80$ m-N/deg + Non-woven
12_3_GCSP4			Geocell (GC4)	4 in. height
12_3_GCSP6			Geocell (GC6)	6 in. height
12_3_BL6_GCSP4			Geogrid (BL6) + Geocell (GCSP4)	$j = 0.98$ m-N/deg + 4 in. height
12_3_BL6_GCSP6			Geogrid (BL6) + Geocell (GCSP6)	$j = 0.98$ m-N/deg + 6 in. height

“Test ID” nomenclature: “Base thickness_CBR of Subgrade_Primary Reinforcement type_Secondary Reinforcement type”

Experimental Program

Large-Scale Repeated Load Testing on Geogrid Reinforcements

Test ID	h	CBR_{sg}	Geosynthetic type	Geosynthetic material property
12_1_UR	12 in.	CBR 1	-	-
12_1_BL5			Geogrid (BL5)	$j = 0.80$ m-N/deg
12_1_BL6			Geogrid (BL6)	$j = 0.98$ m-N/deg
12_1_BL7			Geogrid (BL7)	$j = 1.50$ m-N/deg
12_3_UR		CBR 3	-	-
12_3_BL5			Geogrid (BL5)	$j = 0.80$ m-N/deg
12_3_BL6			Geogrid (BL6)	$j = 0.98$ m-N/deg
12_3_BL7			Geogrid (BL7)	$j = 1.50$ m-N/deg
6_1_UR			6 in.	CBR 1
6_1_BL6	Geogrid (BL6)	$j = 0.98$ m-N/deg		
6_1_BL7	Geogrid (BL7)	$j = 1.50$ m-N/deg		
6_3_UR	CBR 3	-		-
6_3_BL6		Geogrid (BL6)		$j = 0.98$ m-N/deg
6_3_BL7		Geogrid (BL7)		$j = 1.50$ m-N/deg

“Test ID” nomenclature: “Base thickness_CBR of Subgrade_Primary Reinforcement type_Secondary Reinforcement type”

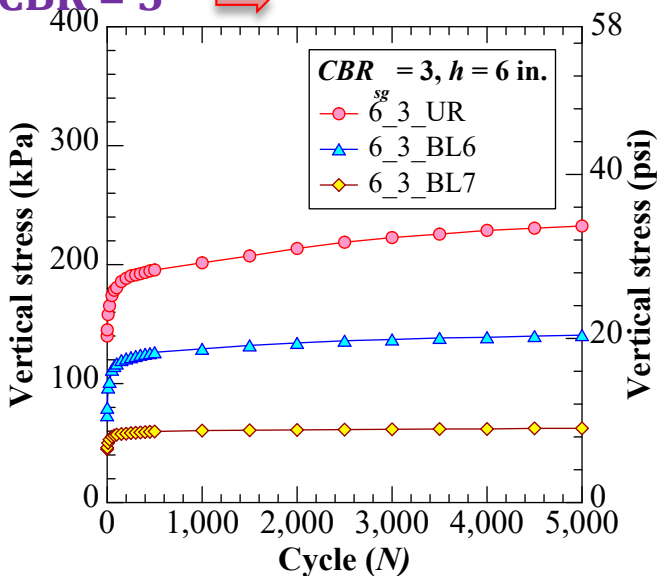
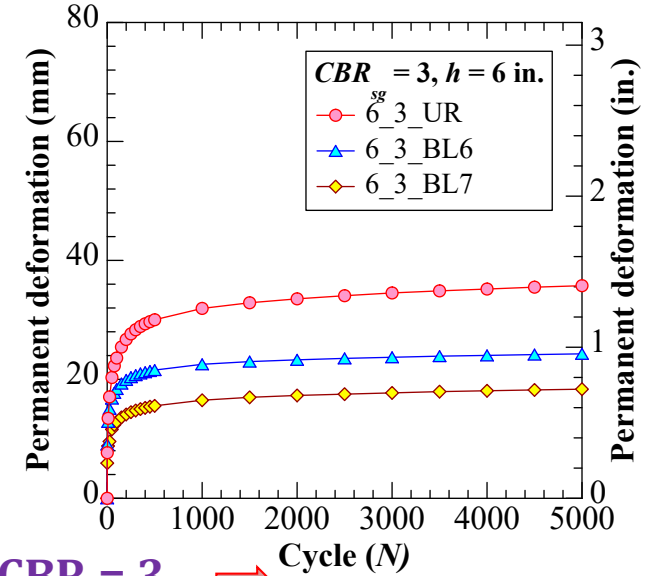
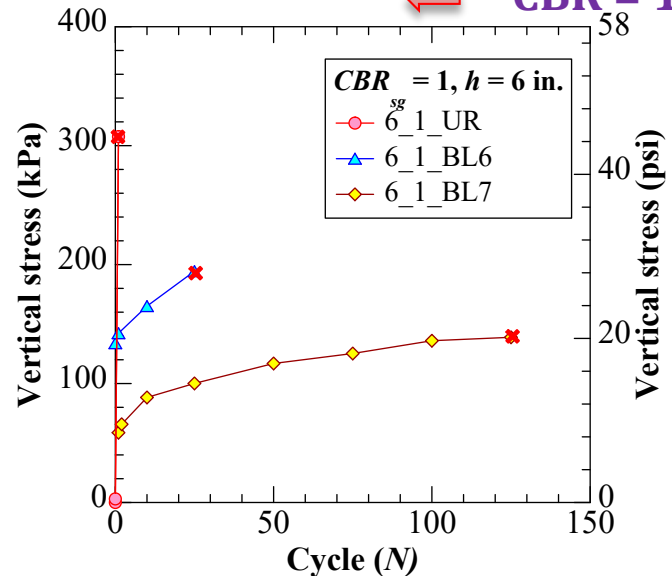
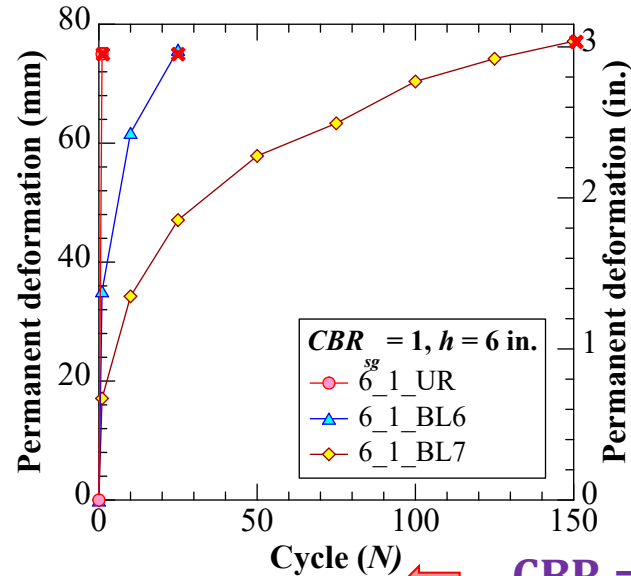
Test Results and Trends

Surface Deformation:

- Permanent deformation ↓ subgrade strength ↑, base thickness ↑ and geogrid stiffness j ↑
- $CBR_{sg} = 1$; 6 in. base layer test sections failed (3 in. or 75 mm) before reaching 150 loading cycles

Vertical stresses

- Vertical stresses at top of subgrade reduced with geosynthetic reinforcement
- The key influencing factors: Geogrid stiffness (j), Subgrade strength (CBR_{sg}), r/h ratio



Unpaved Base Layer Design – Theory

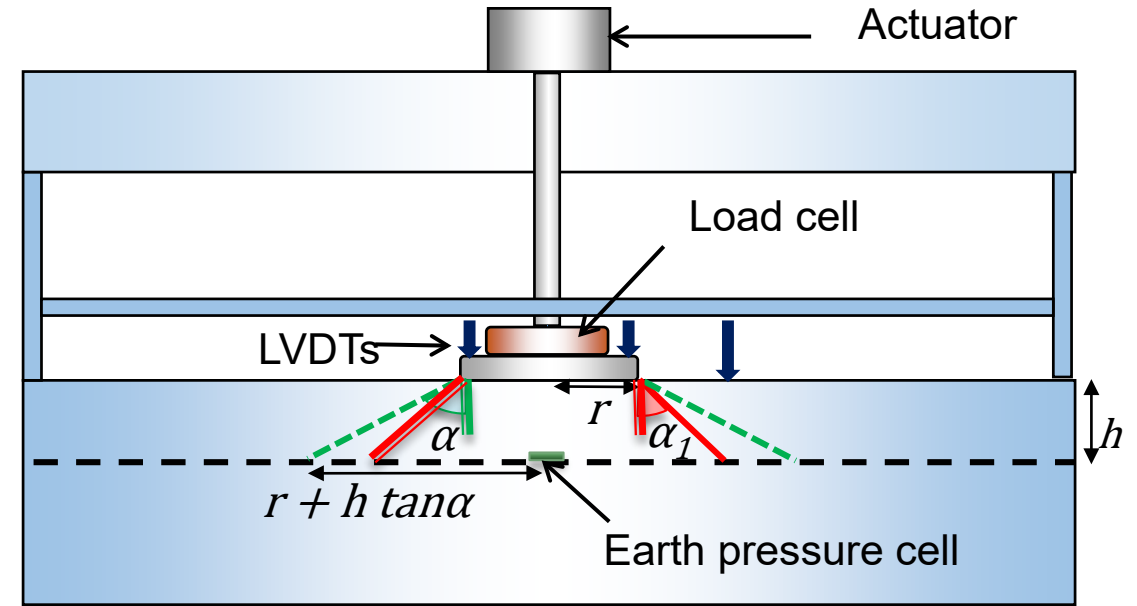
Stress at interface, $p_i = \frac{P}{\pi (r + h \tan \alpha)^2}$

$$h = \frac{1}{\tan \alpha} \times \left(\sqrt{\frac{P}{\pi r^2 p_i}} - 1 \right) \times r$$

Stress on subgrade should be less than mobilized bearing capacity

$$p_i \leq m N_c c_u$$

$$h \geq \frac{1}{\tan \alpha} \left(\sqrt{\frac{P}{\pi r^2 \left(\frac{s}{f_s} \right) \left\{ 1 - 0.9 \exp \left[- \left(\frac{r}{h} \right)^2 \right] \right\} N_c c_u}} - 1 \right) \times r$$



- Initial stress distribution angle, α
- Subsequent stress distribution angle, α_1

Where, P = vehicular load applied, r = the loading plate of radius, h = the thickness of the base layer, α = stress distribution angle, m = bearing capacity mobilization coefficient, N_c = bearing capacity factor; c_u = undrained cohesion of the subgrade soil (kPa), f_s = factor equal to 75 mm rut depth and s = rut depth (mm)

Unpaved Base Layer Design – Theory

Geogrid-reinforced unpaved roads

- Stress distribution angle (α) → improvement with geogrids → generate

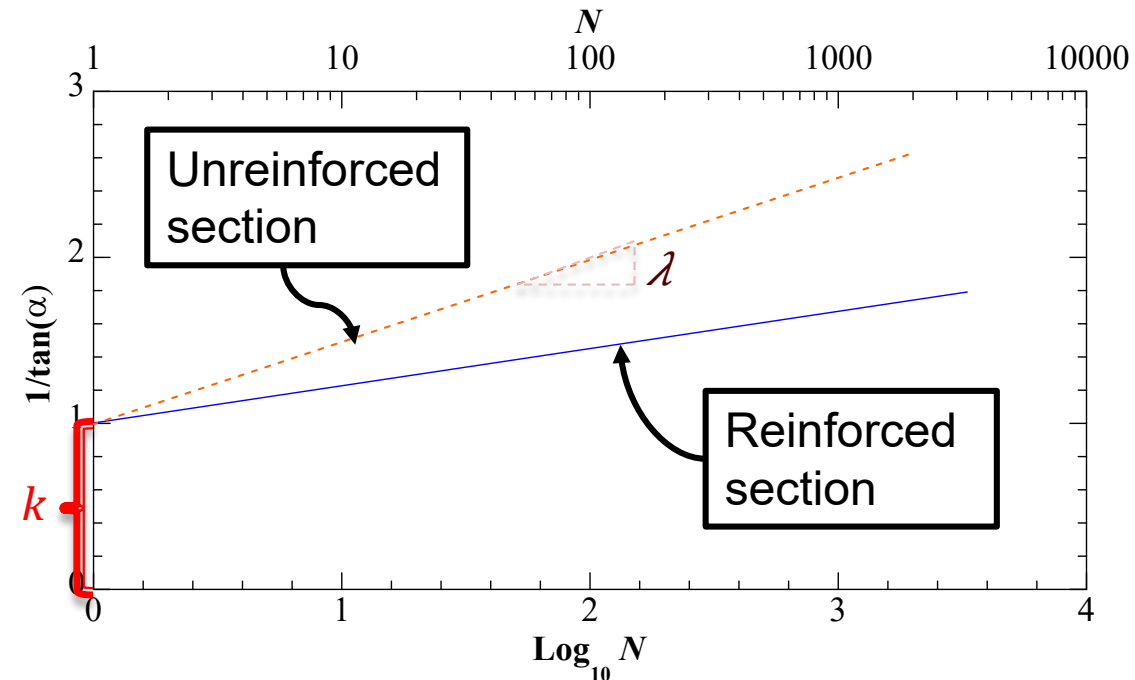
$1/\tan(\alpha)$ vs. $\log_{10}N$ graphs

- Intercept is k and Slope is λ
- Giroud and Han (2004b, 2004a) Method

→ α depends on

- Ratio of loading plate radius to base layer thickness (r/h)
- Types of geosynthetics (j)
- Number of loading cycles (N)
- Parameter k is a constant value of 1.1

$$\frac{1}{\tan(\alpha)} = k + \lambda \times \log_{10}N$$



Unpaved Base Layer Design – Theory

Geogrid-reinforced unpaved roads

- ❑ k is not constant
- ❑ The slope of the line decreases

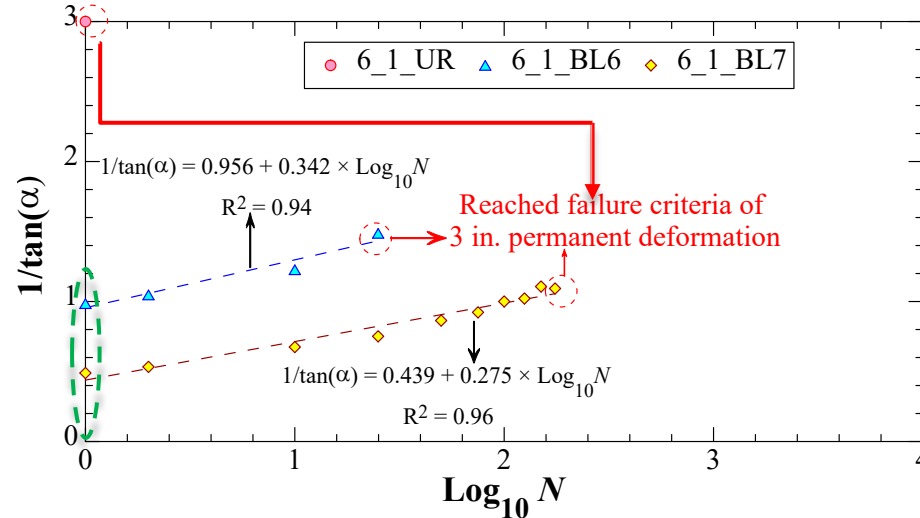
➤ Geogrid stiffness

(j) ↑

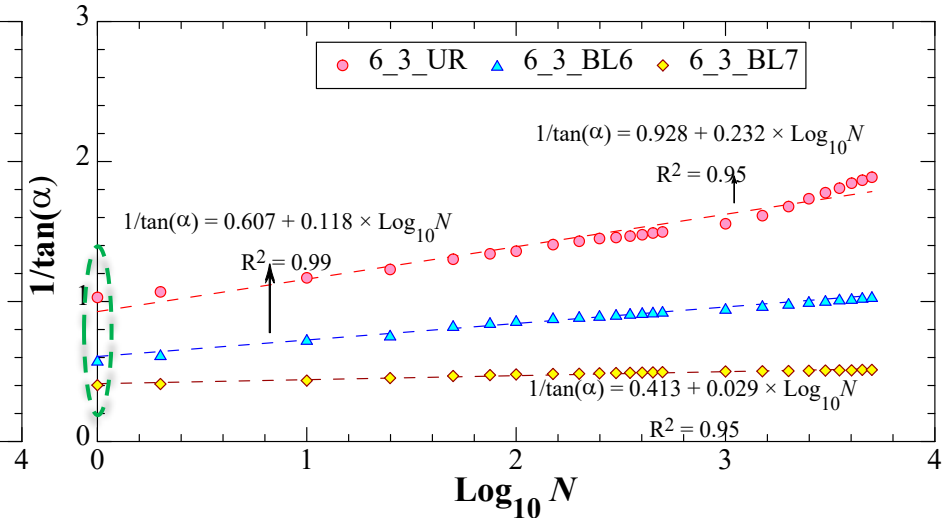
➤ Subgrade

strength (CBR_{sg}) ↑

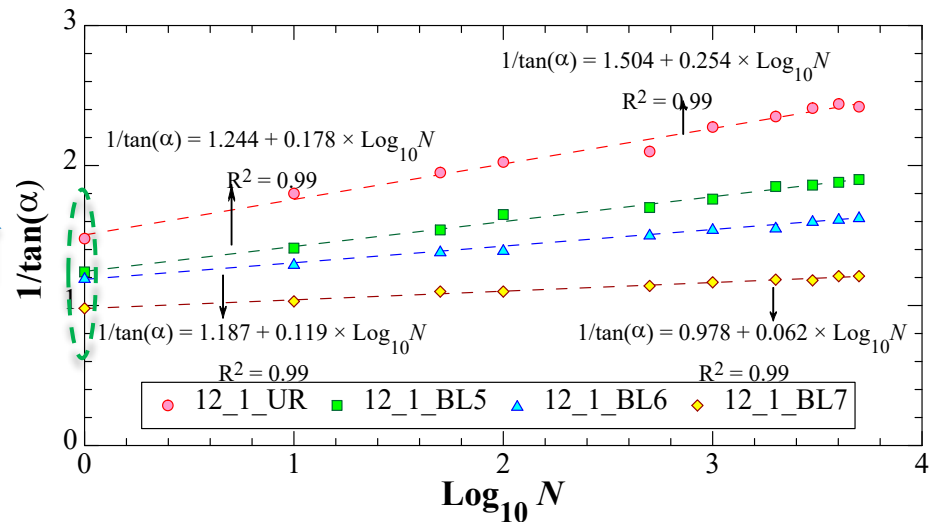
$CBR_{sg} = 1, h = 6$ in.



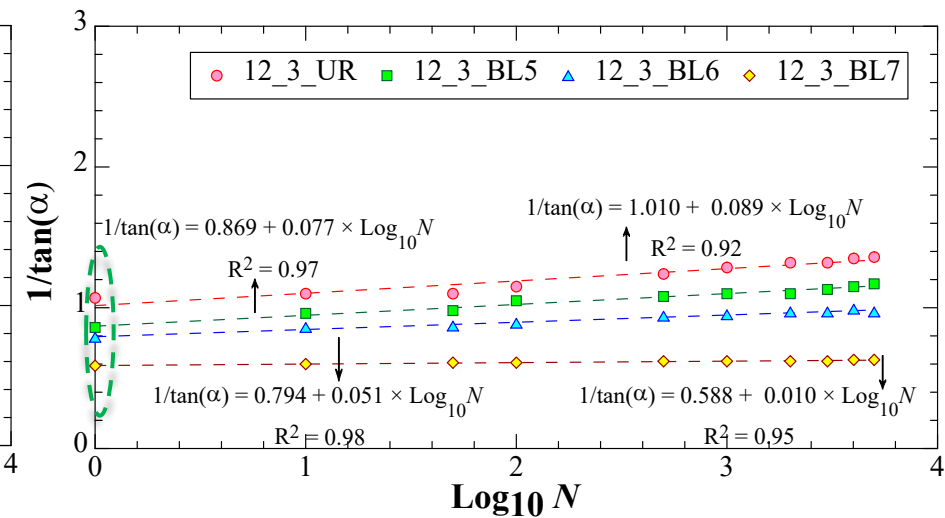
$CBR_{sg} = 3, h = 6$ in.



$CBR_{sg} = 1, h = 12$ in.



$CBR_{sg} = 3, h = 12$ in.



Unpaved Base Layer Design

Base Thickness	Subgrade CBR	Reinforcement Type	λ	k	R^2
6 in.	1	Unreinforced	-	-	-
	1	BL6	0.342	0.956	0.94
	1	BL7	0.275	0.439	0.96
	3	Unreinforced	0.232	0.928	0.95
	3	BL6	0.118	0.607	0.99
	3	BL7	0.029	0.413	0.96
12 in.	1	Unreinforced	0.254	1.504	0.99
	1	BL5	0.178	1.244	0.99
	1	BL6	0.119	1.187	0.99
	1	BL7	0.062	0.978	0.99
	3	Unreinforced	0.089	1.010	0.93
	3	BL5	0.077	0.869	0.97
	3	BL6	0.051	0.794	0.98
	3	BL7	0.010	0.588	0.95



Unpaved Base Layer Design

Effect of different variable on design parameters, (k and λ)

Effect of k

$k \downarrow \Rightarrow$ Geogrid $j \uparrow$

$k \uparrow \Rightarrow$ moduli ratio $R_E \uparrow$

Effect of λ

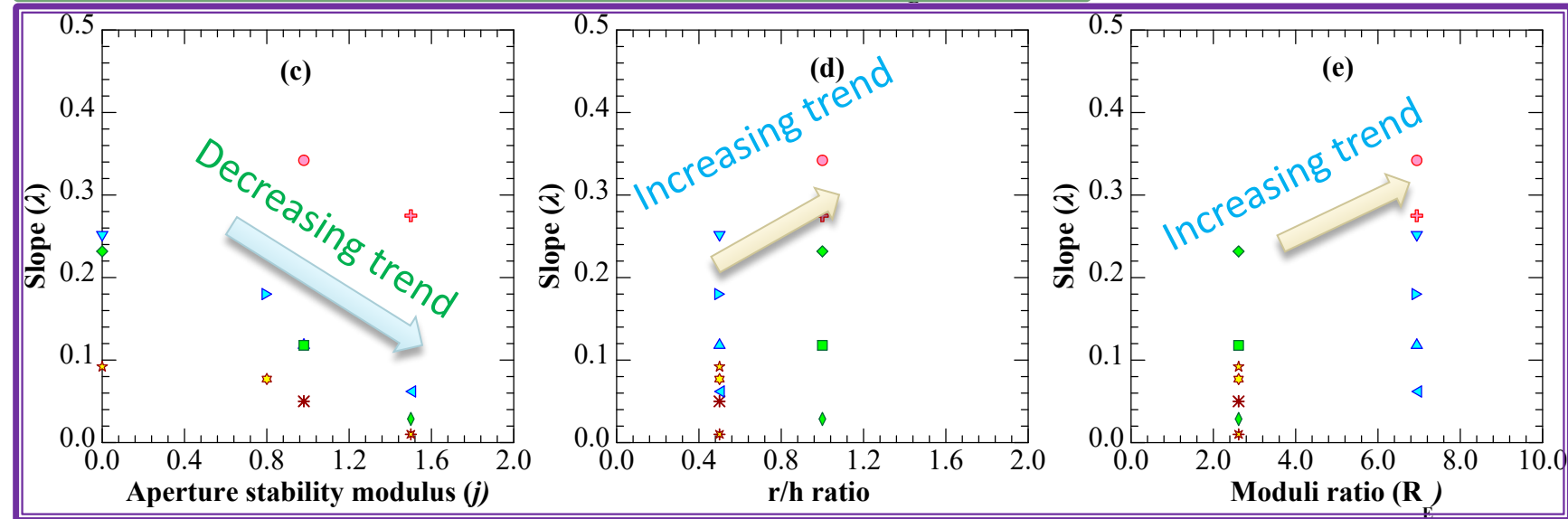
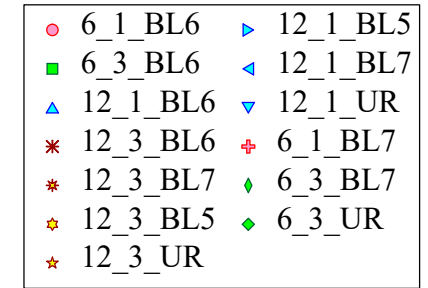
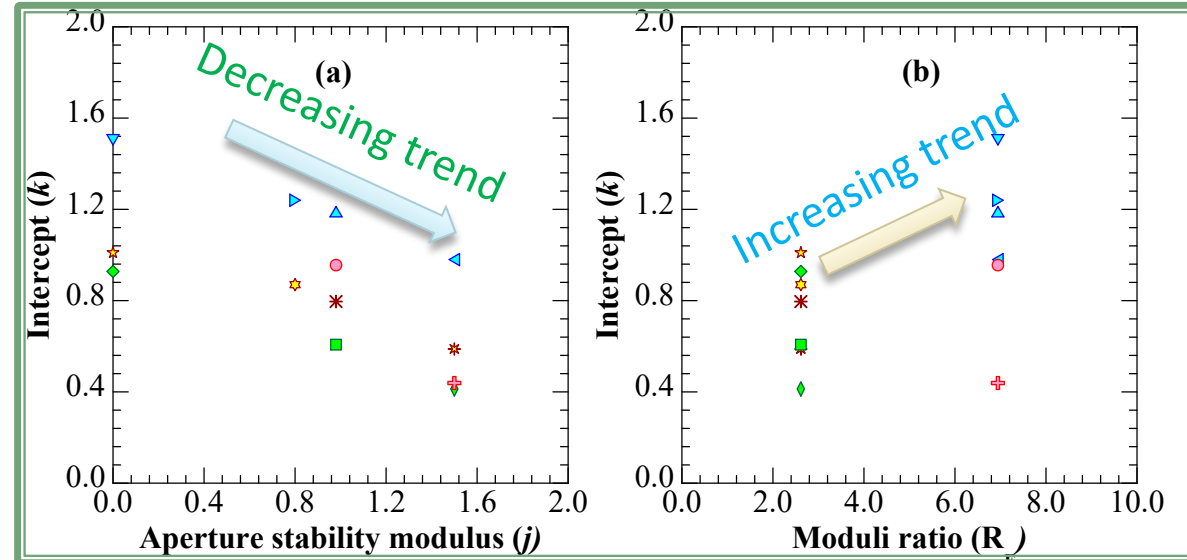
$\lambda \downarrow \Rightarrow$ Geogrid $j \uparrow$

$\lambda \uparrow \Rightarrow$ moduli ratio $R_E \uparrow$

$\lambda \uparrow \Rightarrow$ r/h ratio \uparrow

$$k = f(E_1, E_2, j)$$

$$\lambda = f(E_1, E_2, r, h, j)$$

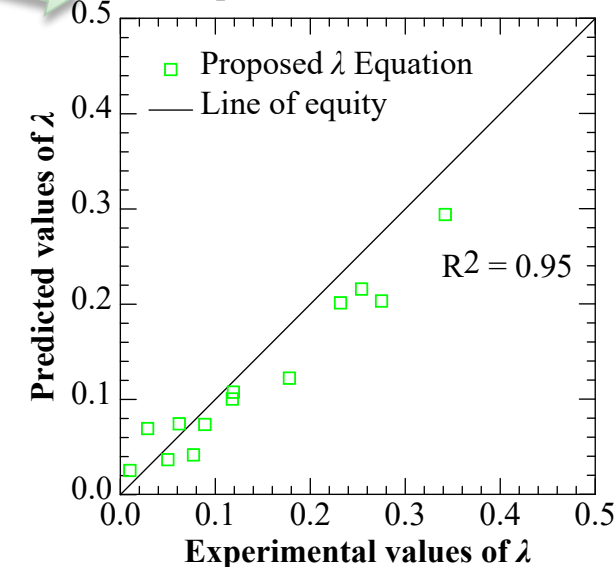
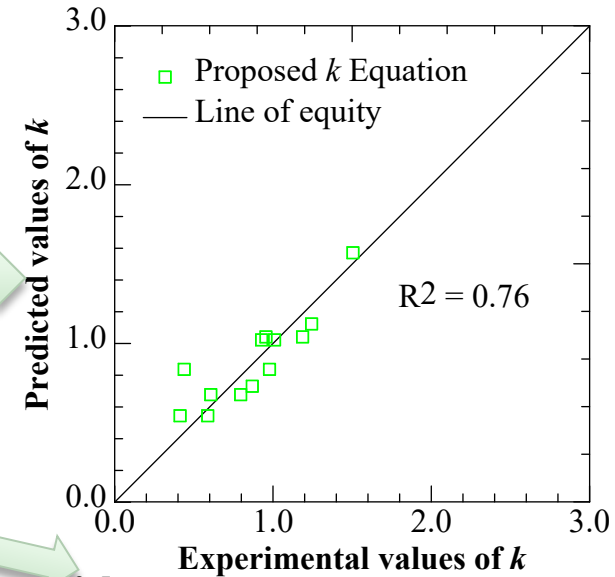


Unpaved Base Layer Design

- The coefficients for k and λ obtained from performing multiple variable regression modeling on the TAMU laboratory test results

$$k = 0.67e^{(-0.42 \times j)} (R_E)^{0.43}; R^2 = 0.76$$

$$\lambda = 0.07e^{(-0.71 \times j)} (R_E)^{1.1} (r/h)^{1.45}, R^2 = 0.95$$



- Generalized form of the $1/\tan(\alpha)$ by substituting k and λ parameters is

$$\frac{1}{\tan \alpha} = [0.67e^{(-0.42 \times j)} (R_E)^{0.43}] + 0.07e^{(-0.71 \times j)} (R_E)^{1.1} (r/h)^{1.45} \times \log_{10} (M)$$

Unpaved Base Layer Design

Proposed Design Equation

$$h_{lab} = \frac{0.67 e^{-0.42 j} (R_E)^{0.43} + (0.07 e^{-0.71 j}) \left(\frac{r}{h}\right)^{1.45} (R_E)^{1.1} \log_{10}(N)}{\{1 + 0.204 [R_E - 1]\}} \left\{ \frac{\frac{P}{(\pi r^2)}}{\sqrt{\left(\frac{s}{f_s}\right) \left\{1 - 0.9 \exp\left[-\left(\frac{r}{h}\right)^2\right]\right\} N_c c_u}} - 1 \right\} \times r$$

- G-H method developed a laboratory to field calibration factor based on field tests conducted by Hammitt (1970). The average value of the field calibration factor (f_{cal}) is 0.69

$$h_{field} = h_{lab} \times 0.69$$

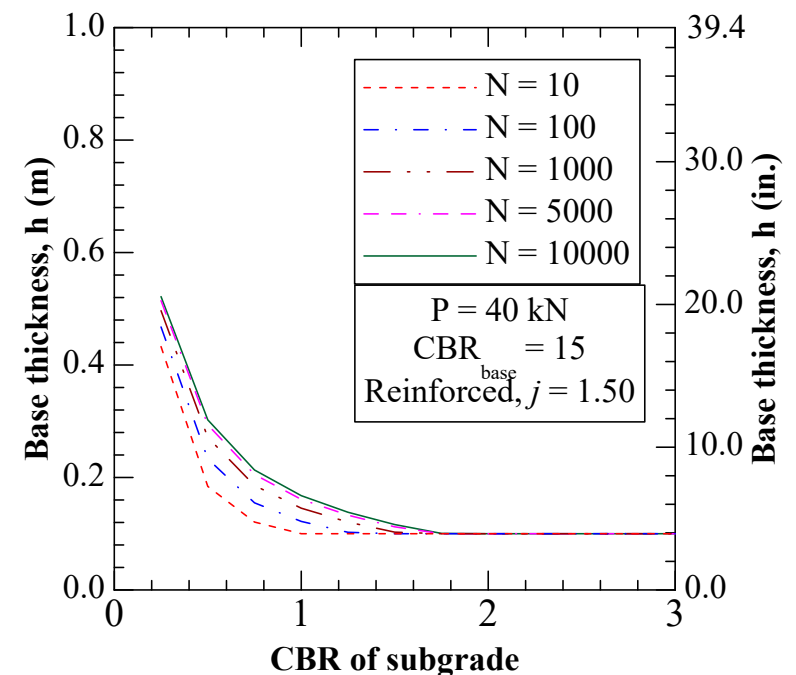
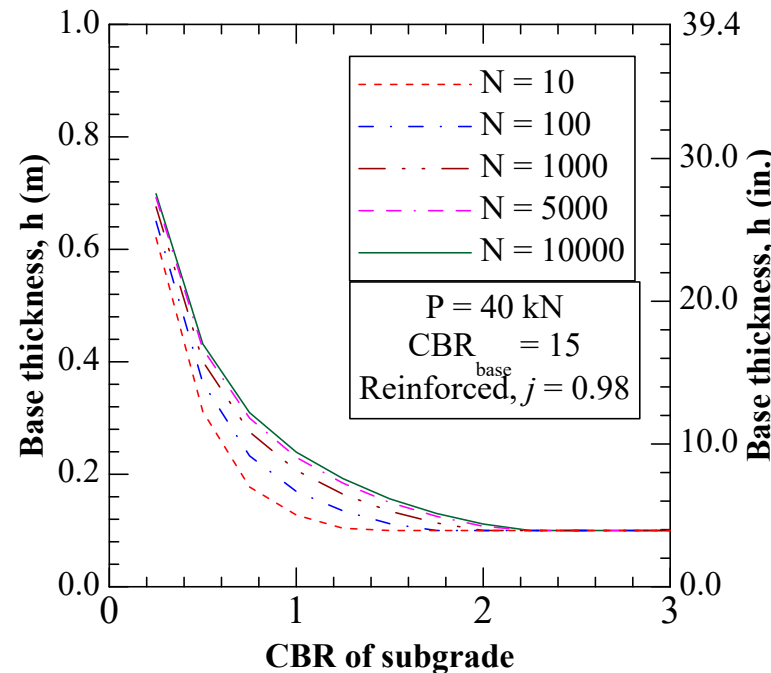
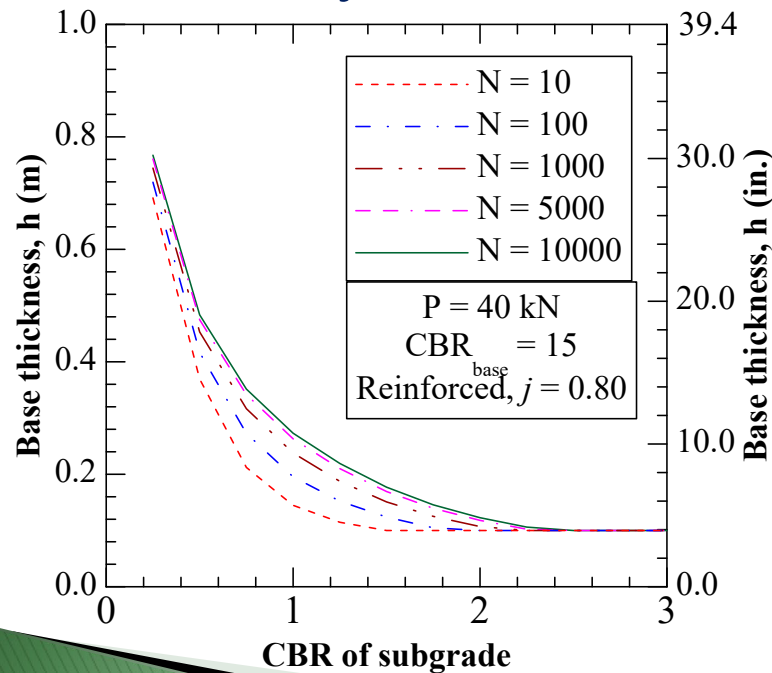
$$h_{field} = \frac{0.46 e^{-0.42 j} (R_E)^{0.43} + (0.048 e^{-0.71 j}) \left(\frac{r}{h}\right)^{1.45} (R_E)^{1.1} \log_{10}(N)}{\{1 + 0.204 [R_E - 1]\}} \left\{ \frac{\frac{P}{(\pi r^2)}}{\sqrt{\left(\frac{s}{f_s}\right) \left\{1 - 0.9 \exp\left[-\left(\frac{r}{h}\right)^2\right]\right\} N_c c_u}} - 1 \right\} \times r$$

Note: Further validation with full-scale field testing on high stiffness geogrids of IFI may yield different calibration factor.

Design Charts

Proposed Design Charts

- ❑ Design charts shows base thickness for a range of subgrade strength (CBR_{sg}) and for different loading cycles for different geogrids with different j properties
- ❑ A minimum base thickness of 6 in. is recommended when the design equation in the chart yields thickness lower than 6 in.



Limitations

- The current proposed design method's validity is limited to the assumptions made and the testing conditions followed in the research
 - Proposed design methodology validity is constrained to testing variables:
 - ❖ R_E values ranging between 2.6 to 6.9
 - ❖ CBR values of subgrade soils within the range of 1 and 3
 - ❖ Biaxial geogrids with j values ranging from 0.8 m-N/deg to 1.5 m-N/deg
 - Developed equation → for stiff subgrade yields lower design base thickness, < 6 in. → Recommend a **minimum thickness of 6 in.** for practical considerations and insights from the laboratory data.
 - **An average field calibration factor of 0.69 (from previous design methods) was followed**
 - **Future field studies on high strength materials may yield different field calibration factors**

Summary

- ❑ Current laboratory studies showed the addition of geosynthetics significantly enhances the performance of the unpaved section sections constructed on weak subgrades.
- ❑ G-H equation has been updated to include stiffer geogrids and the proposed method is recommend for geogrids with j values ranging from 0.8 m-N/deg to 1.5 m-N/deg
- ❑ Design charts were developed for IFI geosynthetic products

Future Works

- ❑ Field testing and long-term performance of the high modulus geogrids
- ❑ For paved layer coefficients, we recommend large box test on 3-layered system with upper layer simulating asphalt concrete

Performance of pavement sections with H₂Ri geosynthetics

Project Leader: Nripojyoti Biswas

Team members: Avinash Gonnabathula, Krishneswar Ramineni
and Gustavo Hernandez Martin

PI: Anand J. Puppala

Professor | A.P. and Florence Wiley Chair

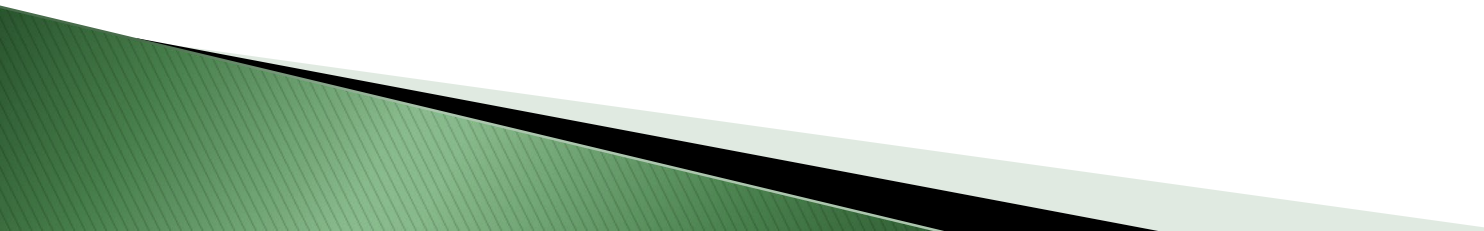
Director – Center for Infrastructure Renewal

Closed Meeting

TAMU Site Proprietary

NSF IUCRC CICI TAMU SITE
NSF IUCRC CICI - IAB Spring 2024 Meeting

Presentation Outline

- ❖ **Introduction**
 - ❖ **Task Plan**
 - ❖ **Life Cycle Analysis**
 - ❖ **Field Test Sections**
 - ❖ **Large Scale Lab testing**
 - ❖ **Summary**
- 

Introduction

❖ Objective

- ❑ Evaluate the feasibility/efficiency of using H₂Ri geosynthetic for improving drainage and strength of pavement sections built on high-plastic expansive soil

❖ Field Studies indicated efficacy of application

❖ Laboratory studies

- ❑ Control Section
- ❑ Reinforced Sections



Control Section



Reinforced Section

Task Plan

Task 1

✓ Literature Review

✓ Geomaterial
Characterization

✓ Construction of Test Sections

✓ Instrumentation and Monitoring

Task 2

✓ Laboratory Studies
(H₂Ri)

✓ Wicking Tests

✓ Parametric Study

Task 3

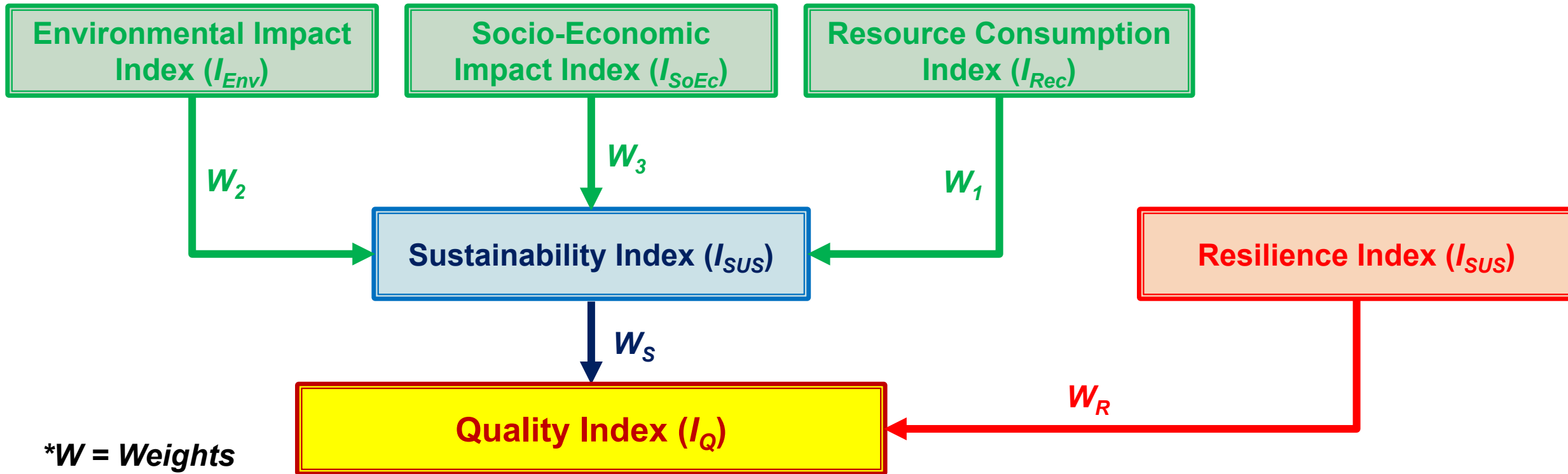
Life Cycle Analysis

Carbon Footprint
Analysis

Design & Construction
Guidelines

Life Cycle Analysis

Combined Assessment Framework (Das 2018)



* W = Weights

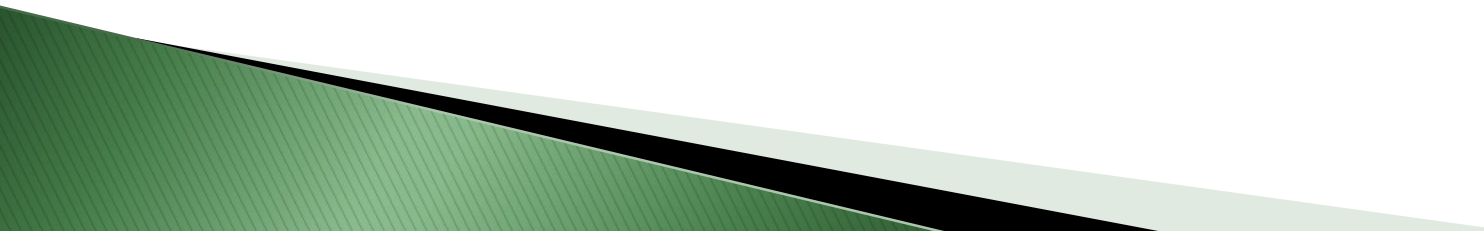
* $\sum W = 1$

$$I_{SUS} = W_1 \times I_{Env} + W_2 \times I_{SoEc} + W_3 \times I_{Rec}$$

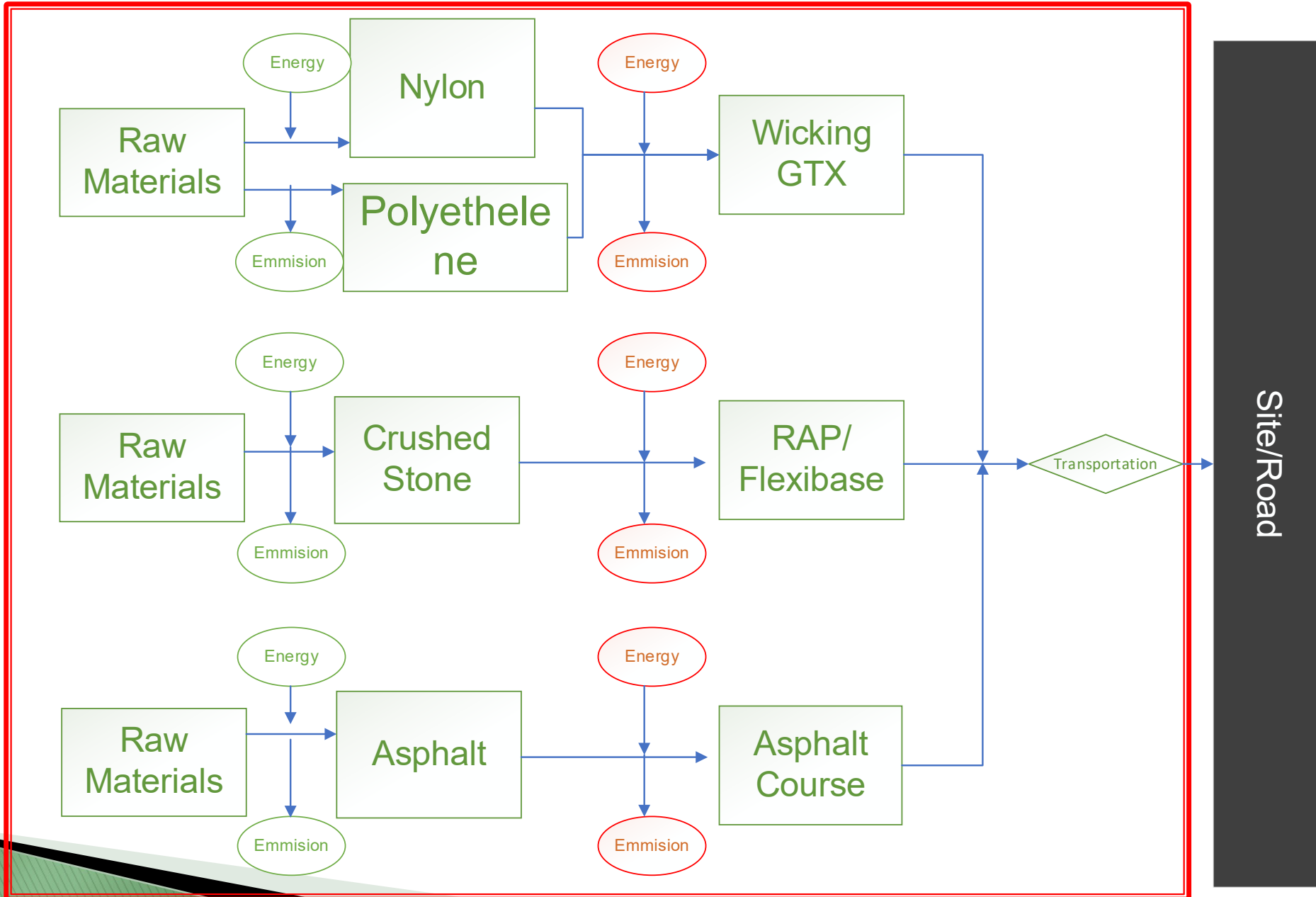
$$I_Q = W_s \times I_{SUS} + W_R \times I_{Res}$$

Lower value
indicates better
alternative

Life Cycle Analysis Outline

- ❖ **Boundary condition is considered as cradle to gate + transportation to site**
 - ❖ **Construction machinery costs and impacts are ignored**
 - ❖ **The database costs are market costs for the products**
 - ❖ **Cost and Impact analysis was done per meter length of road**
 - ❖ **Sustainability analysis for environmental impact was performed using OpenLCA**
 - ❖ **ReCiPe 2016 Midpoint method was used for calculation**
- 

Process Flow



Sustainability Analysis – Test Parameters

$$I_{Rec} = w_{1a} \times E_E (\text{material production}) + w_{1b} \times E_E (\text{Transportation})$$

$$I_{Env} = w_2 \times GW_P$$

$$I_{SoEc} = w_3 \times C$$

Where,

w_i = Weight factors

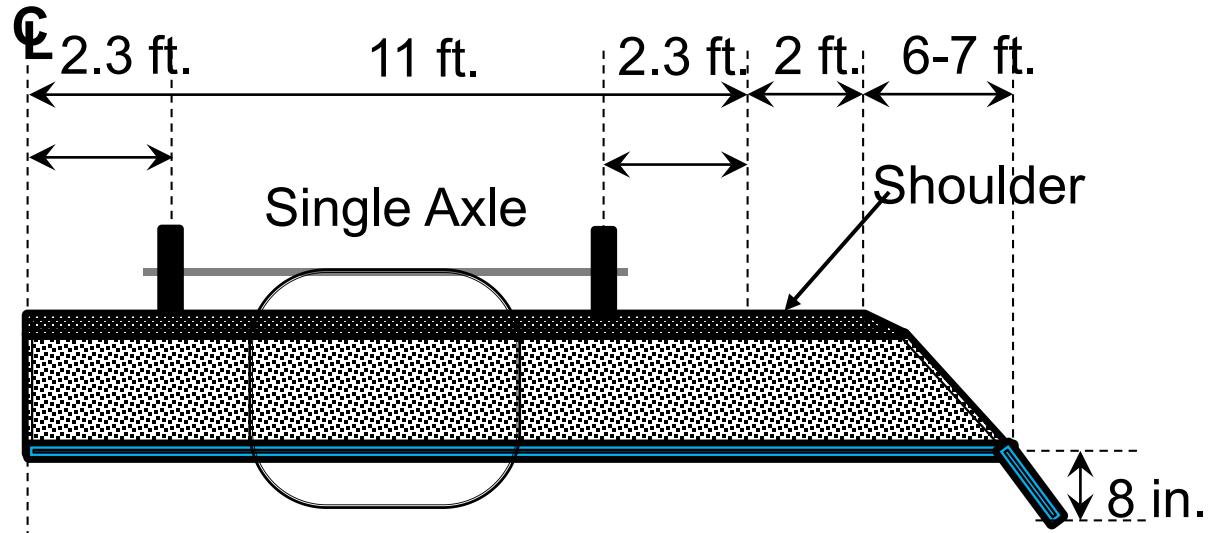
E_E = Embodied Energy

GW_P = Global Warming Potential

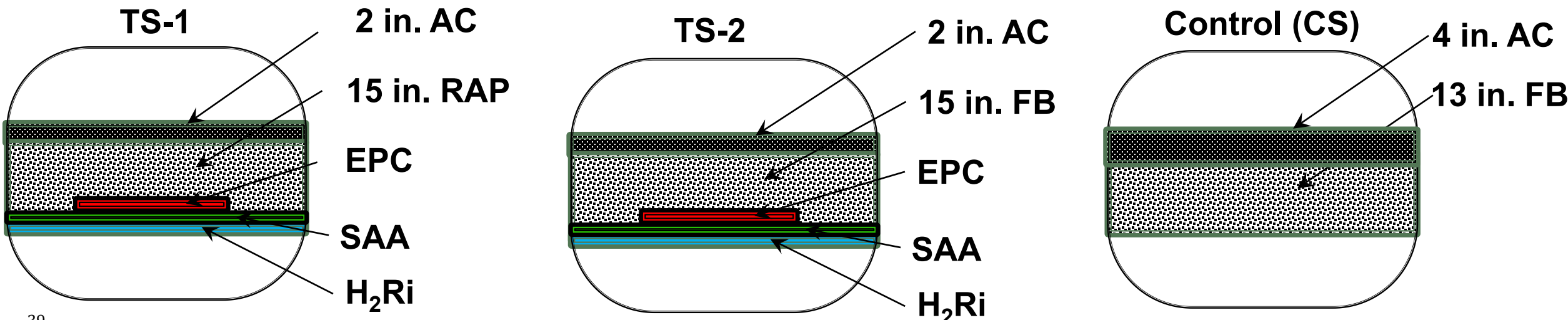
C = Cost of the process

Test ID	A	B	C
Section ID	TS-1	TS-2	Control
Section Parameters	15 in. RAP + 2 in. AC + H ₂ Ri gtx	15 in. FB + 2 in. AC + H ₂ Ri gtx	13 in. FB + 4 in. AC
Section Length	3.3 m	3.3 m	3.3 m
Section Width	15 ft.	15 ft.	15 ft.

Field Test Sections – FM1807 Venus, Texas



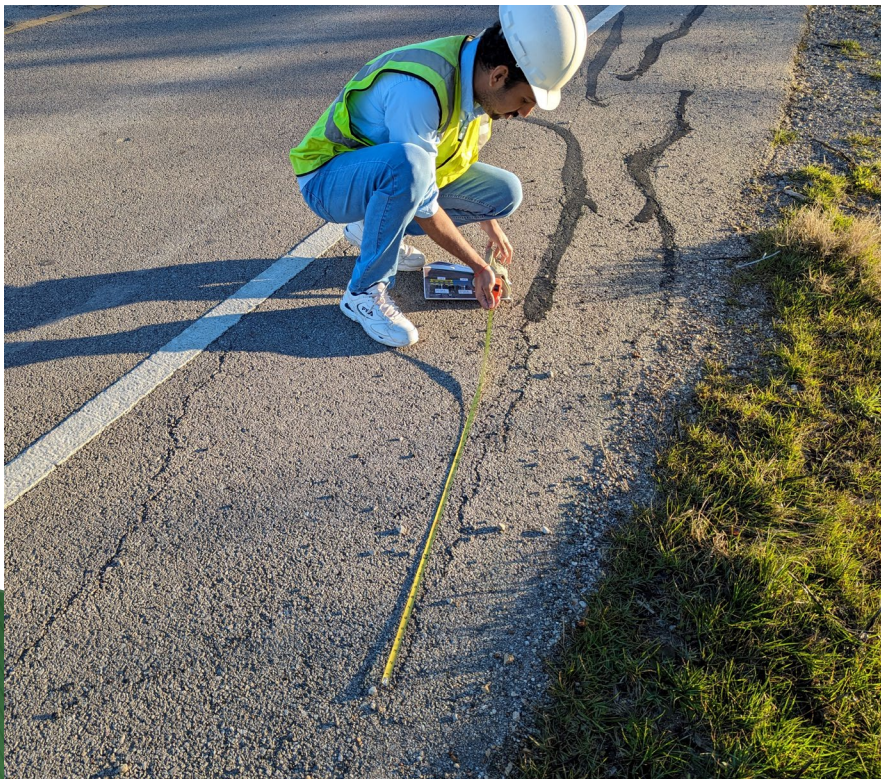
AC – Asphalt Concrete RAP - Reclaimed Asphalt Pavement Aggregates FB - Flex Base
 EPC - Earth Pressure Cells SAA - Shape Array Sensors



Field Test (In-situ Observations)

- ❖ Section A & B shows no surface distresses except for some cracks on shoulders.
- ❖ Section C has some visible distresses on the outer wheel path.

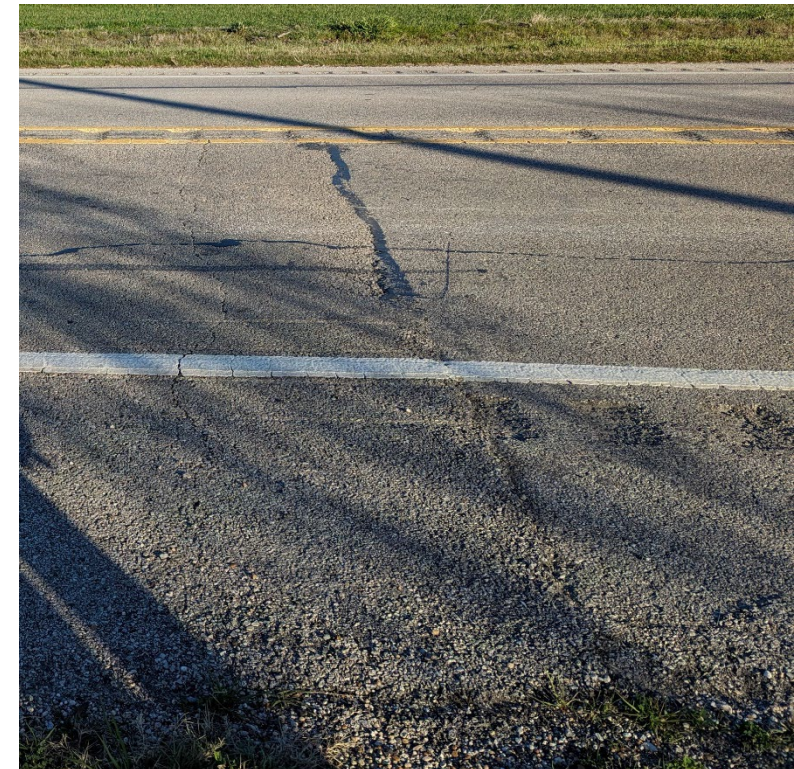
Section A



Section B



Section C



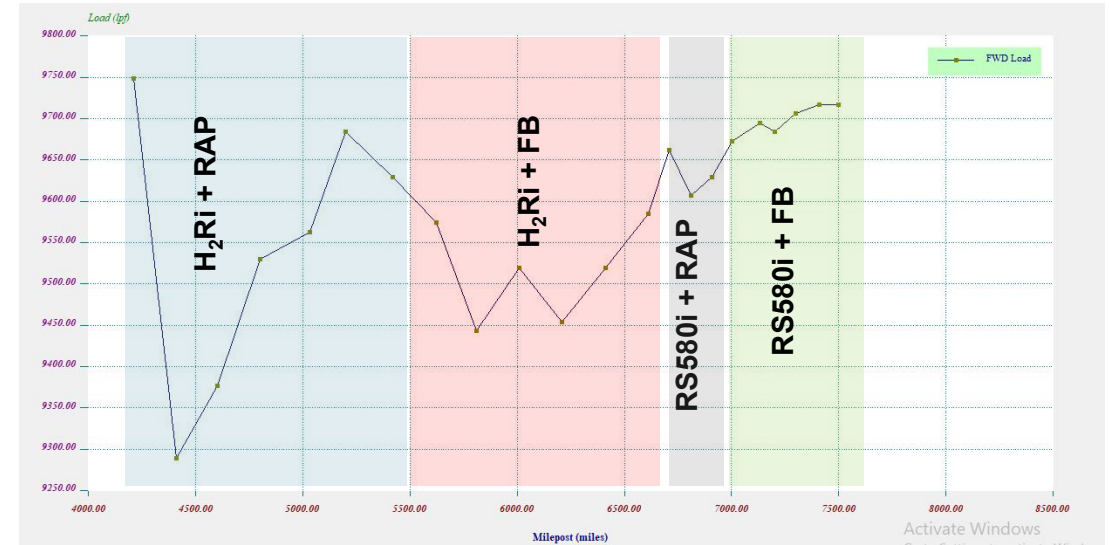
Falling Weight Deflectometer Tests – February 2024

Drop Weight at each Station (lbf)

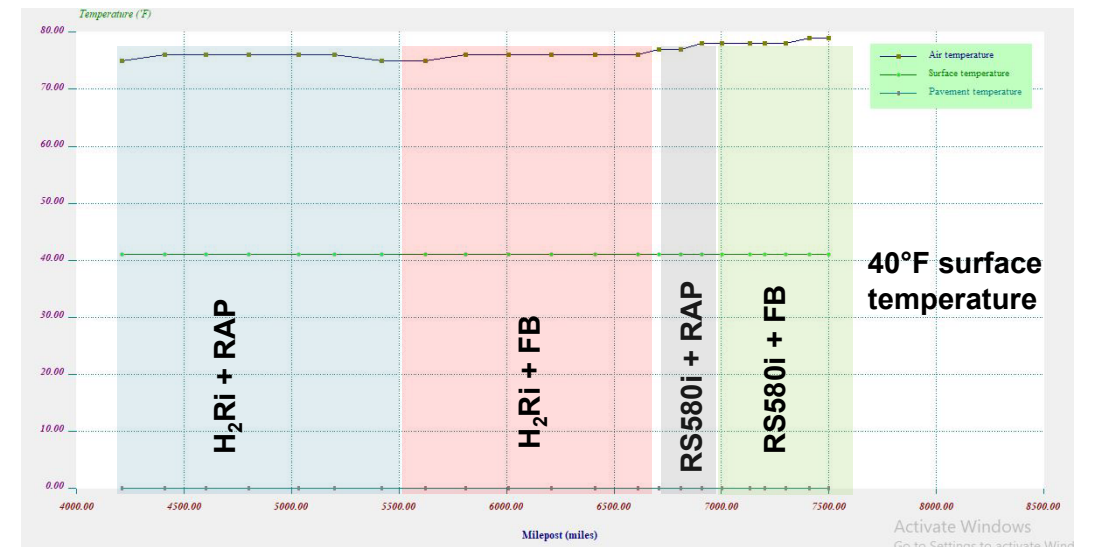


FWD Test on Field Test Sections

❖ Deformations measured using 7 sensors (D1-D7)

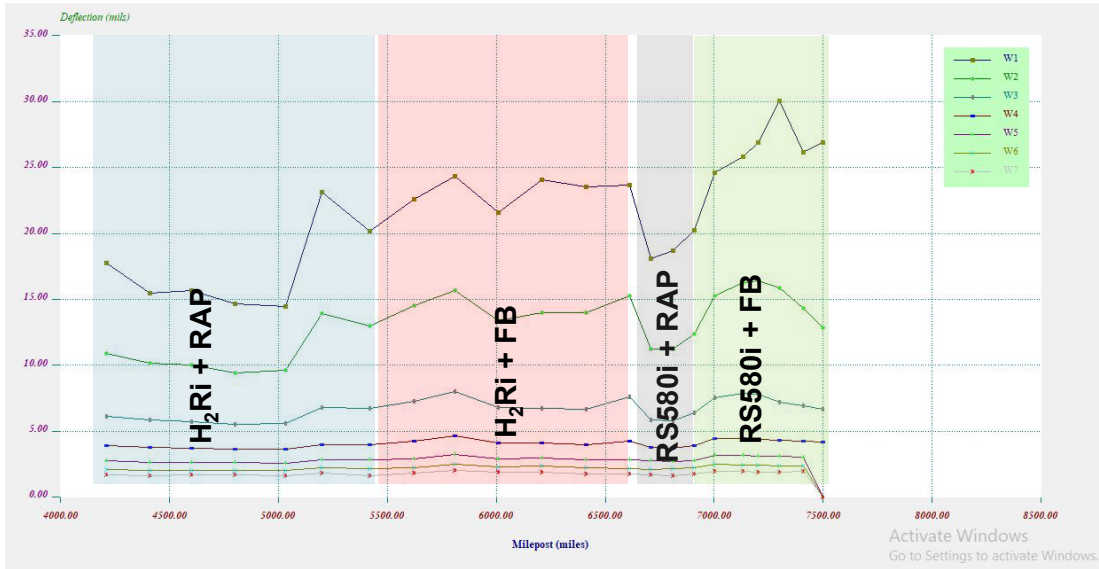


Pavement and Air Temperature

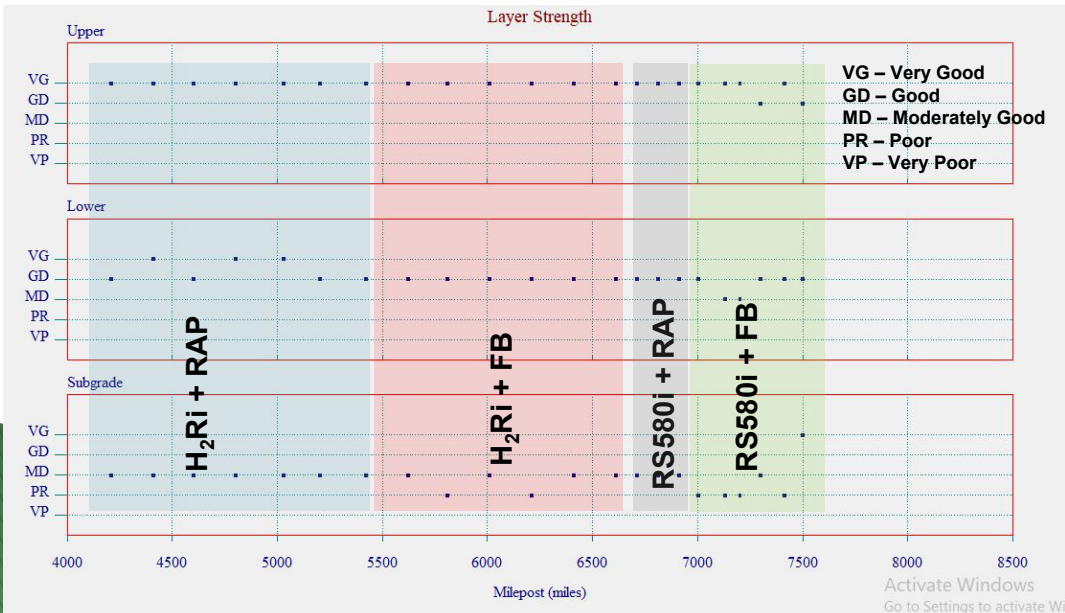


Falling Weight Deflectometer Tests - Results

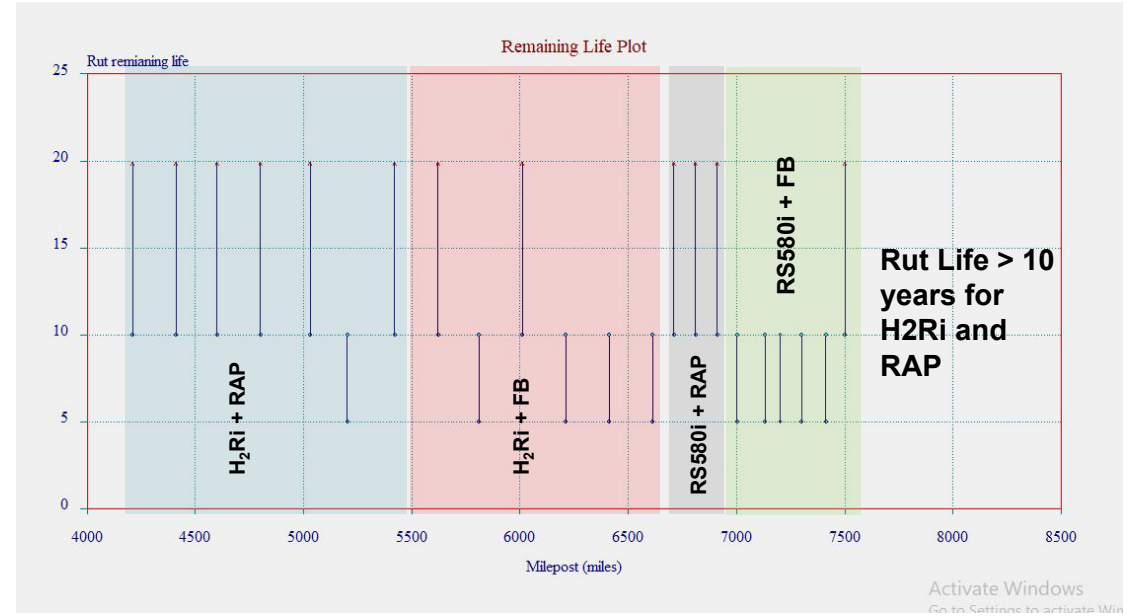
Deformation for sensors (D1-D7)



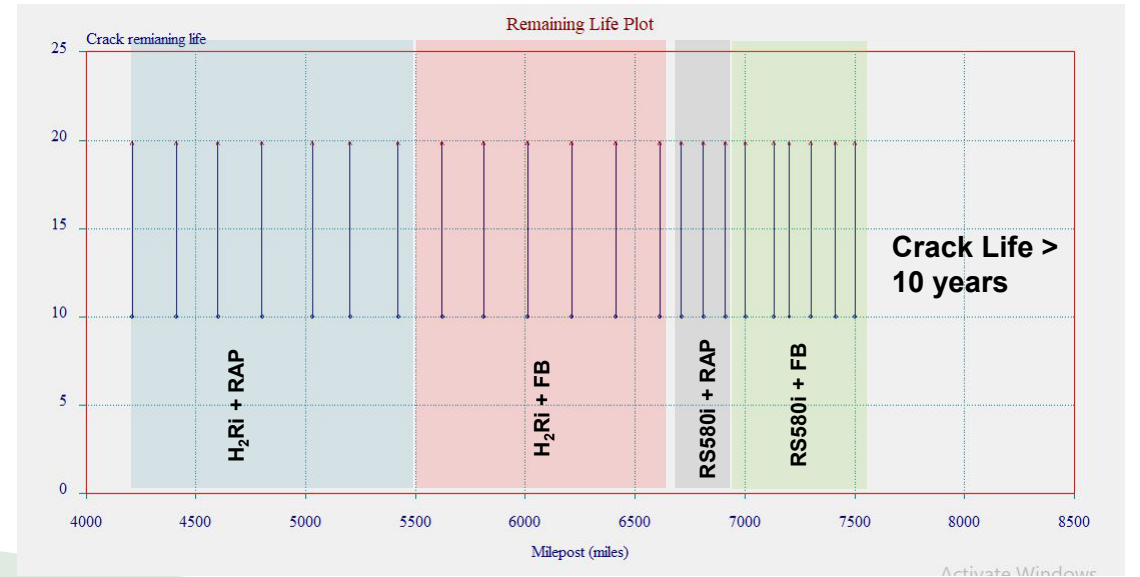
Layer Conditions



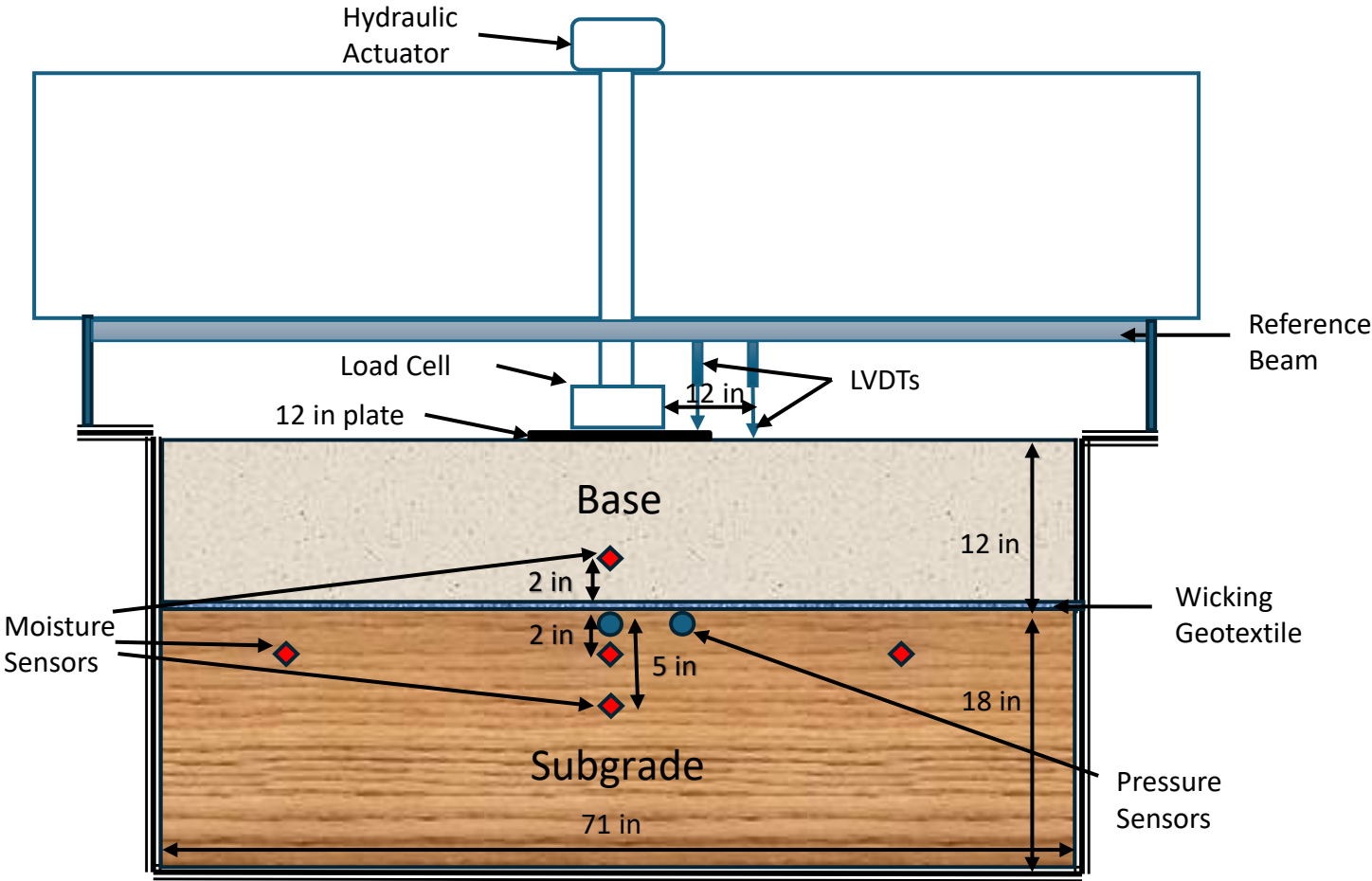
Remaining Rut-Life



Remaining Crack-Life

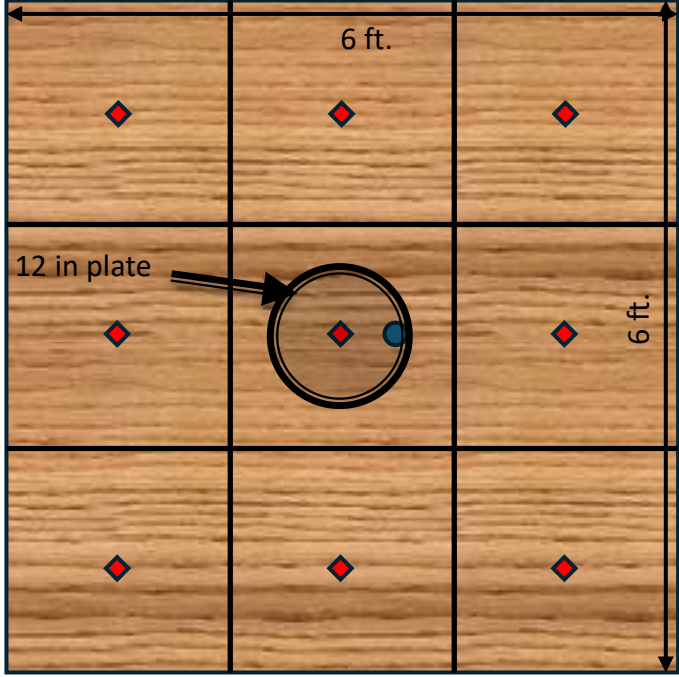


Schematic of Large Box Setup



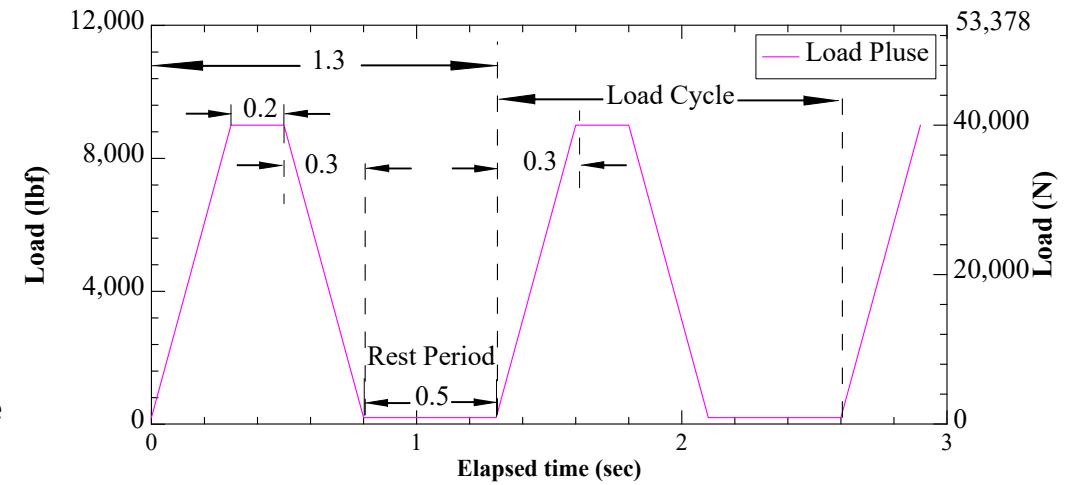
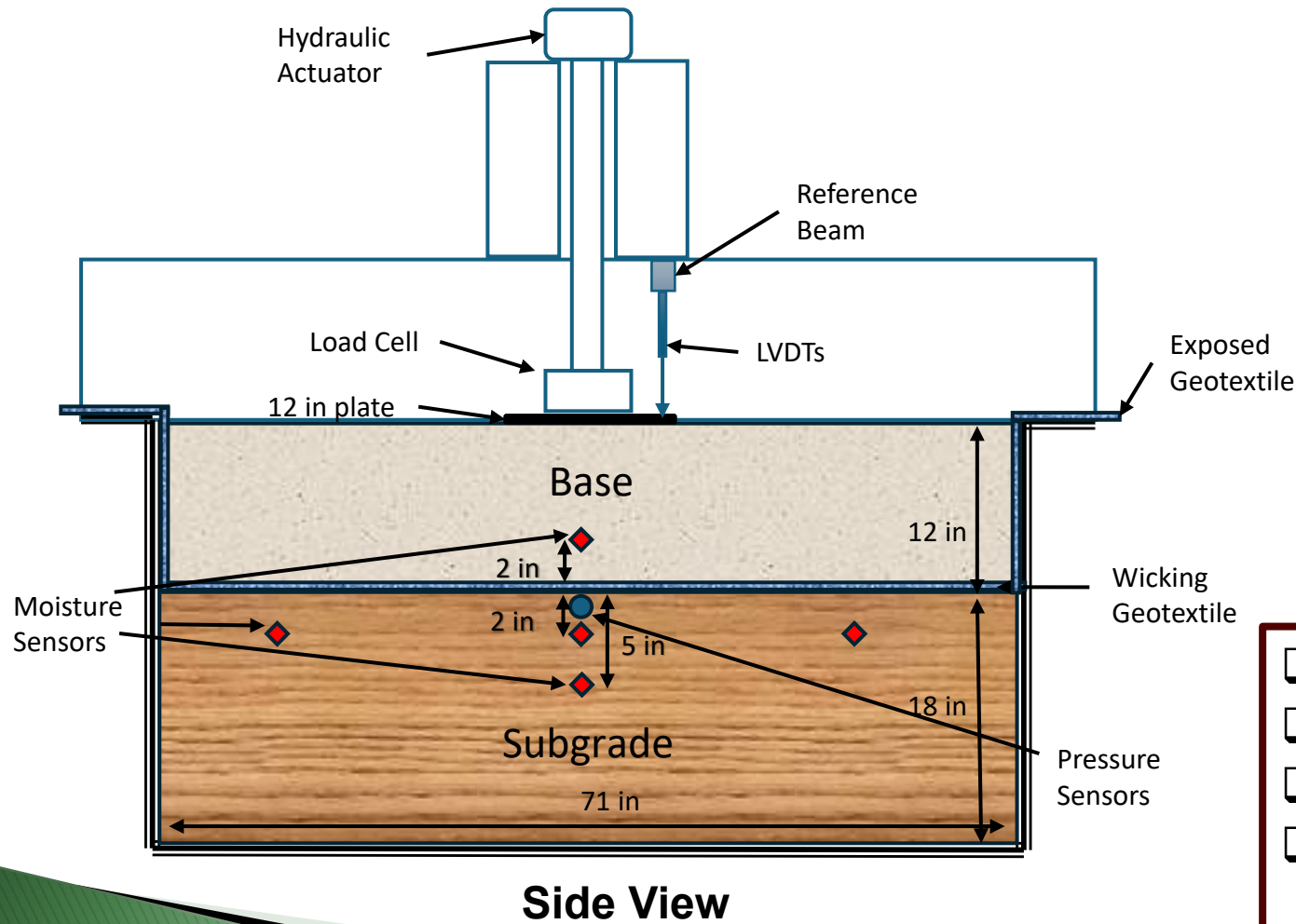
Front View

- ◆ Moisture Sensors
- Pressure Sensors



Top View

Schematic of Large Box Setup



Repeated load pulse

- ❑ Frequency of loading: 0.77 Hz
- ❑ Peak load: 9000 lbf
- ❑ Loading plate diameter: 12 in.
- ❑ Instrumentation: Load cell, pressure sensors, Multiple LVDTs and strain gauges

Box Construction

- ❖ The box will be filled with subgrade and compacted in layers after mixing the soil at OMC and saturated after the construction
- ❖ Geotextile → interface of subgrade and base layers
- ❖ The test sections will be equipped with moisture sensors and LVDTs
- ❖ Quality control during construction:
 - Soil core specimens will be collected
 - Variable energy dynamic cone penetration test (VE-DCP) or traditional DCP
 - Light Weight Deflectometer (LWD) tests are performed



Box Preparation

- ❖ The box is waterproofed at the bottom from the inside and geo membrane is installed for additional protection.



Load Cell



Geo Membrane

Future Works

- ❖ **Need to develop a comprehensive Life Cycle Cost Analysis (LCCA) for the H2Ri geotextile (cradle-to-gate + End-of-life)**
- ❖ **Large Scale Testing is to be performed.**